

CP violation in the HZZ vertex and left-right asymmetries

A. I. Hernández-Juárez^{1,*} and R. Gaitán¹

¹*Departamento de Física, FES-Cuautitlán, Universidad Nacional Autónoma de México, C.P. 54770, Estado de México, México.*

(Dated: February 3, 2025)

We calculate new contributions to the HZZ vertex from the Flavor Changing Neutral Current (FCNC) of the Higgs and Z bosons. It is found that the h_2^V and h_3^V ($V = H, Z$) form factors can be induced through these couplings, and we present our results in terms of the Passarino-Veltman scalar functions. Using the current limits on $H\bar{t}c$ and $Z\bar{t}c$ couplings, we determine that the new contributions to the CP -conserving form factor h_2^V are small in comparison to the Standard Model (SM) predictions. However, for the CP -violating form factor h_3^V , the contributions can reach values as large as 10^{-6} , five orders of magnitude larger than in the SM. Furthermore, we examine how these results influence the left-right asymmetries in the processes $H^* \rightarrow ZZ$ and $Z^* \rightarrow ZH$. Our findings indicate that significant deviations from the SM predictions may arise when FCNC contributions are considered.

I. INTRODUCTION

In the SM of particle physics, the Higgs boson, discovered in 2012 at the Large Hadron Collider (LHC) [1, 2], is the remnant of the Brout-Englert-Higgs mechanism that gives mass to the gauge bosons and fermions [3–5]. Since the Higgs boson discovery, notable progress has been made in measuring its properties [6, 7]. Recently, the couplings of the Higgs boson with weak bosons have attracted considerable attention, mainly due to the LHC reported the signal strength of the $H \rightarrow Z\gamma$ decay that is twice the SM expectation [8, 9]. Furthermore, for the first time, the evidence of a pair of Z bosons produced via an off-shell Higgs boson was announced by the ATLAS and CMS collaborations [10, 11]. This finding also facilitated the determination of Γ_H by analyzing the ratio between the on-shell and off-shell Z pair production rates [12, 13]. Moreover, the HZZ vertex has also been proposed to be sensitive to quantum entanglement effects at the LHC [14–18].

The HZZ vertex with anomalous couplings can be induced through the following effective Lagrangian

$$\mathcal{L} = \frac{g}{c_W} m_Z \left[\frac{(1 - a_Z)}{2} H Z_\mu Z^\mu + \frac{1}{2m_Z^2} \left\{ \hat{b}_Z H Z_{\mu\nu} Z^{\mu\nu} + \hat{c}_Z H Z_\mu \partial_\nu Z^{\mu\nu} + \tilde{b}_Z H Z_{\mu\nu} \tilde{Z}^{\mu\nu} \right\} \right], \quad (1)$$

where a_Z corresponds to the tree-level correction, while \hat{b}_Z arises at the one-loop level within the SM and is of order 10^{-2} [19–21]. The anomalous coupling \hat{c}_Z is also expected to emerge at the one-loop level; however, it has not been identified yet in SM calculations. The a_Z , \hat{b}_Z and \hat{c}_Z couplings are CP -conserving [19], whereas \tilde{b}_Z is CP -violating and could be generated at the three-loop level in the SM, with an approximate magnitude of 10^{-11} [22]. Stringent bounds on \hat{c}_Z and \tilde{b}_Z were established through LHC data and theoretical calculations, which are of order $10^{-2} - 10^{-4}$ [21]. The phenomenology of the H^*ZZ coupling at the LHC and future colliders has been extensively studied by numerous authors [23–29]. Additionally, the cases HZZ^* and HZ^*Z^* have relevant implications at colliders [30–49]. The $H^* \rightarrow ZZ$ decay is included in publicly available codes such as HDECAY [50] and PROPHECY4F [51].

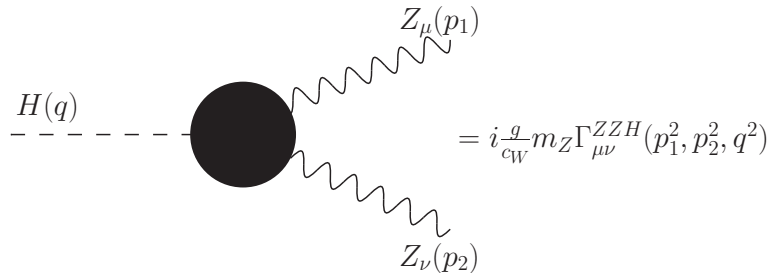


FIG. 1. Nomenclature for the HZZ coupling and the $\Gamma_{\mu\nu}^{ZZH}$ vertex function.

* alan.hernandez@cuautitlan.unam.mx

From Lagrangian 1 and using the nomenclature in Fig 1, the vertex function can be written as follows

$$\Gamma_{\mu\nu}^{ZZH} = h_1^V(q^2, p_1^2, p_2^2)g_{\mu\nu} + \frac{h_2^V(q^2, p_1^2, p_2^2)}{m_Z^2}p_{1\nu}p_{2\mu} + \frac{h_3^V(q^2, p_1^2, p_2^2)}{m_Z^2}\epsilon_{\mu\nu\alpha\beta}p_1^\alpha p_2^\beta, \quad (2)$$

where V denotes the off-shell boson. Following the kinematics $H^* \rightarrow ZZ$ ($Z^* \rightarrow ZH$), the form factors h_i^V can be expressed as

$$h_1^V(q^2, p_1^2, p_2^2) = 1 + a_Z - \hat{b}_Z \frac{q^2 - p_1^2 - p_2^2}{m_Z^2} + \frac{\hat{c}_Z}{2m_Z^2}p_1^2 + p_2^2, \quad (3)$$

$$h_2^V(q^2, p_1^2, p_2^2) = \pm 2\hat{b}_Z, \quad (4)$$

$$h_3^V(q^2, p_1^2, p_2^2) = \pm 2\tilde{b}_Z. \quad (5)$$

For simplicity, we will set $a_Z = 0$ in this work. Since we consider an off-shell V boson, the anomalous couplings are functions of the squared four-moment of the V boson. Moreover, given that \hat{b}_Z has an imaginary part in the SM [21], we also expect that $\hat{c}_Z, \hat{b}_Z, \tilde{b}_Z$ will be complex quantities. It is important to note that Lagrangian in Eq. (1) necessitates real anomalous couplings to be Hermitian; however, it merely describes the external particles through an effective approach, which is only valid at Born level [52]. The anomalous couplings are induced by heavy or light particles at the one-loop or higher orders [32], where the operators that induce such corrections do not strictly require real $\hat{c}_Z, \hat{b}_Z, \tilde{b}_Z$ couplings to form a Hermitian Lagrangian. The imaginary part, together with the CP -violating form factor, may give rise to intriguing new physics effects that could be observed through polarized observables at the LHC [21, 36, 53–56]. The phenomenology involving a pair of polarized Z bosons in the process $pp \rightarrow H^* \rightarrow ZZ$ at the LHC has been addressed in Refs. [57–61]. The polarizations of gauge bosons are particularly noteworthy at the LHC and are currently under investigation across various processes. For instance, the ATLAS collaboration has reported evidence of longitudinally polarized $W^\pm Z$ and ZZ boson pairs [62, 63]. Additionally, polarization fractions of the Z bosons have been analyzed by the LHCb, ATLAS, and CMS collaborations [64–67]. Studies involving gauge boson polarizations at the LHC include $W^\pm W^\pm$ production [68], W +Jets events [69, 70], $W^\pm Z$ production [71], and the generation of W bosons in $t\bar{t}$ events and top decays [72–75]. The potential for producing polarized gauge bosons has been incorporated into event generators like MadGraph5_aMC@NLO [76] and SHERPA [77].

In this study, we examine the FCNC contributions of the Higgs and Z bosons to the HZZ vertex, with a particular focus on those that induce the CP -violating form factor h_3^V ($V = H, Z$). Furthermore, we investigate the potential for new left-right asymmetries arising from the polarizations of the Z -bosons. The structure of this work is organized as follows: in Sec. II, we calculate the new contributions to the HZZ vertex resulting from FCNC couplings mediated by the H and Z bosons. Next, in Sec. III, we analyze the left-right asymmetries that can be induced by the CP -violating form factor h_3^V . Finally, in Sec. IV, we present a numerical analysis of our results, with our conclusions summarized in Sec. V.

II. FCNC CONTRIBUTIONS TO THE HZZ COUPLING

To generate CP -violating contributions to the HZZ vertex, we consider the following effective Lagrangian, which induces FCNC couplings mediated by the Z and H bosons

$$\mathcal{L} = \frac{g}{c_W} \bar{f}_j \gamma_\mu \left(g_V^{ij} - g_A^{ij} \gamma^5 \right) f_i Z^\mu - \frac{g}{2m_W} H \bar{f}_j \left(g_S^{ij} + g_P^{ij} \gamma^5 \right) f_i, \quad (6)$$

where g_r^{ij} ($r = V, A, S, P$) are complex couplings. Given its large mass, we expect the most significant contributions from FCNC interactions involving the top quark. Such processes have been investigated at the LHC through the decays $t \rightarrow Zq$ and $t \rightarrow Hq$ [78, 79]. In the SM, the corresponding branching ratios are highly suppressed, with $\mathcal{B}(t \rightarrow Zq)$ being of order 10^{-14} . For $\mathcal{B}(t \rightarrow Hq)$, the prediction is even smaller, by about one order of magnitude [80]. Constraints on the couplings $Z\bar{t}q$ and $H\bar{t}q$ ($q = c, u$) have been obtained from LHC data [81, 82], which can be summarized as follows:

$$|g_V^{tc}|, |g_A^{tc}| \leq 0.0095, \quad (7)$$

$$|g_S^{tc}|, |g_P^{tc}| \leq 1.2 \text{ GeV}. \quad (8)$$

In the rest of this section, we will calculate the one-loop FCNC contributions to the h_2^V and h_3^V from factors arising from Lagrangian (6). We will consider scenarios that involve an off-shell Higgs boson or an off-shell Z boson, with the following kinematics $H^* \rightarrow ZZ$ and $Z^* \rightarrow ZH$.

A. Analytical results

Two distinct contributions to the HZZ vertex can arise from the FCNC couplings in Lagrangian (6). The first category of diagrams (Type I), as illustrated in Fig. 2, involves only flavor-violating couplings mediated by the Z boson. The second category (Type II) also includes FCNC couplings of the Higgs boson and is depicted in Fig. 3. For our calculations, we consider additional diagrams arising from both $p_1^\mu \leftrightarrow p_2^\nu$ and $m_i \leftrightarrow m_j$ exchanges. Our results were obtained using the FeynCalc package [83–86] and are expressed in terms of the Passarino-Veltman scalar functions.

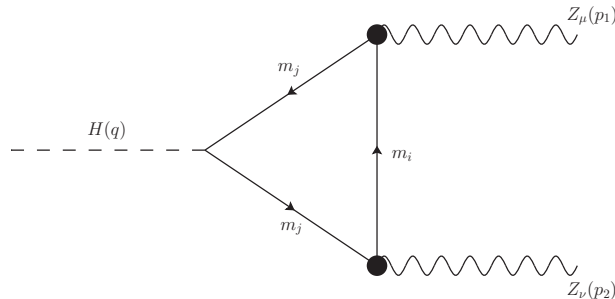


FIG. 2. One-loop contributions of Type I, where only FCNC couplings of the Z boson are involved.

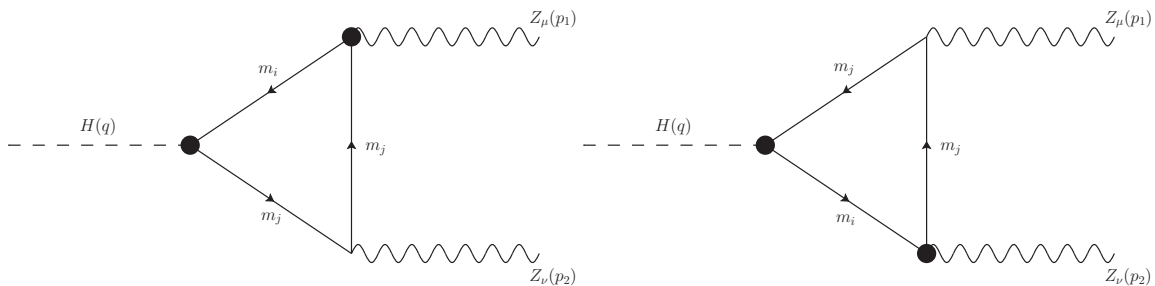


FIG. 3. One-loop contributions of Type II, where FCNC couplings of the Z and H bosons are involved.

1. Diagrams Type I

By considering all the contributing Feynman diagrams from Fig. 2, we obtained the FCNC contribution to the CP -conserving form factor h_2^V , which can be expressed as

$$h_2^V(I) = -\frac{g^2 m_Z N_f}{4\pi^2 c_W m_W} \left\{ |g_V^{ij}|^2 A_V^V(K^2, m_i^2, m_j^2) + |g_A^{ij}|^2 A_A^V(K^2, m_i^2, m_j^2) \right\}, \quad V = H, Z, \quad K = Q, P, \quad (9)$$

where N_f corresponds to the number of colors, and the $A_{V,A}^V$ ($V = H, Z$) functions can be found in Appendix A 1. For the off-shell H case, $A_{V,A}^H$ depends on Q , which is defined as $Q \equiv \|q\|$. In the case of the off-shell Z boson, we define $P = \|p_1\|$, and $A_{V,A}^Z$ will be a function of P . When $m_j = m_i$, the form factor h_2^V ($V = H, Z$) reduces to twice the SM results [21]. This outcome occurs because, in our calculations, we considered the double of the diagrams due to the $m_i \leftrightarrow m_j$ exchange.

For the CP -violating form factor h_3^V , the FCNC contribution of type I is given as follows

$$h_3^V(I) = -\frac{g^2 m_i m_j m_Z N_f}{2\pi^2 c_W m_W} \text{Im} \left[g_V^{ij} g_A^{ij*} \right] \tilde{\mathcal{F}}^V(K^2, m_i^2, m_j^2), \quad V = H, Z, \quad K = Q, P, \quad (10)$$

where the functions $\tilde{\mathcal{F}}^V$ ($V = H, Z$) can also be found in Appendix A 1. Notably, at least one imaginary coupling in the $Z\bar{f}_j f_i$ vertex is essential for inducing CP violation in the HZZ vertex. For $m_j = m_i$, the form factor h_3^V vanishes.

Moreover, we anticipate negligible contributions for FCNC involving only light fermions, as h_3^V is proportional to the product $m_i m_j$.

The $A_{V,A}^V$ and $\tilde{\mathcal{F}}^V$ ($V = H, Z$) functions in Eqs.(9) and (10) are free of divergences.

2. Diagrams Type II

From diagrams of Type II in Fig. 3, the resulting CP -conserving form factor can be expressed as

$$h_2^V(II) = -\frac{g^2 m_Z N_f}{2\pi^2 c_W m_W} \left\{ g_V \text{Re} \left[g_V^{ij} g_S^* \right] R_1^V(K^2, m_i, m_j) + g_A \text{Re} \left[g_V^{ij} g_P^* \right] R_2^V(K^2, m_i, m_j) \right. \\ \left. + g_A \text{Re} \left[g_A^{ij} g_S^* \right] R_3^V(K^2, m_i, m_j) + g_V \text{Re} \left[g_A^{ij} g_P^* \right] R_4^V(K^2, m_i, m_j) \right\}, \quad V = H, Z, \quad K = Q, P, \quad (11)$$

where g_V and g_A correspond to the SM vector and axial couplings of the Z boson with fermions. The functions R_i^V ($i=1, 2, 3, 4$) are presented in Appendix A2. When $m_j = m_i$, $g_S = m_i$, and $g_P = 0$, our expression simplifies to four times the SM contribution. This result is expected, as we have considered additional Feynman diagrams from the $m_i \leftrightarrow m_j$ and $Z\bar{f}_j f_i$ exchange.

The form factor associated with CP violation can be expressed as follows:

$$h_3^V(II) = \frac{g^2 m_Z N_f}{2\pi^2 c_W m_W} \left\{ g_A \text{Im} \left[g_V^{ij} g_S^* \right] T_1^V(K^2, m_i, m_j) + g_V \text{Im} \left[g_V^{ij} g_P^* \right] T_2^V(K^2, m_i, m_j) \right. \\ \left. + g_V \text{Im} \left[g_A^{ij} g_S^* \right] T_3^V(K^2, m_i, m_j) + g_A \text{Im} \left[g_A^{ij} g_P^* \right] T_4^V(K^2, m_i, m_j) \right\}, \quad V = H, Z, \quad K = Q, P. \quad (12)$$

The functions T_i^V ($i=1, 2, 3, 4$) in Eq. (12) are also shown in Appendix A2. Notably, the pseudoscalar coupling is not required to induce CP -violation. Furthermore, for $g_P = 0$ and $m_j = m_i$, the form factor h_3^V vanishes, whereas for $g_P \neq 0$ the $T_{2,4}^V$ functions are not zero. Therefore, generating CP violation without FCNC couplings remains possible if we include a pseudoscalar coupling. The R_i^V and T_i^V ($i=1,2,3, 4$) functions in Eqs. (11) and (12) are free of divergences.

In summary, we have derived new contributions to the form factor h_3^V ($V = H, Z$) arising from FCNC couplings of the Z and Higgs bosons. These results suggest the possibility of new sources of CP violation in the HZZ vertex, which can lead to left-right asymmetries in the $H^* \rightarrow ZZ$ process [21, 56]. Additionally, our calculations for the CP -conserving form factor are consistent with the SM results for $m_j = m_i$.

III. LEFT-RIGHT ASYMMETRIES OF THE HZZ VERTEX

The polarized observables of the HZZ vertex have been explored in multiple contexts [21, 36, 55, 56], where the left-right asymmetry \mathcal{A}_{LR}^H for the $H^* \rightarrow ZZ$ process is defined as follows:

$$\mathcal{A}_{LR}^H = \frac{\Gamma_{H^* \rightarrow Z_L Z_L}^L - \Gamma_{H^* \rightarrow Z_R Z_R}^R}{\Gamma_{H^* \rightarrow Z_L Z_L}^L + \Gamma_{H^* \rightarrow Z_R Z_R}^R}. \quad (13)$$

By considering the form factors h_i^H as complex, the \mathcal{A}_{LR}^H asymmetry has been computed in Ref. [21], which expressed in terms of the real and imaginary h_1^H and h_3^H is

$$\mathcal{A}_{LR}^H = 4m_Z^2 \mathcal{K}(Q) \frac{\text{Re}[h_1^H] \text{Im}[h_3^H] - \text{Re}[h_3^H] \text{Im}[h_1^H]}{\mathcal{K}^2(Q) \left\{ \text{Re}[h_3^H]^2 + \text{Im}[h_3^H]^2 \right\} + 4m_Z^4 \left\{ \text{Re}[h_1^H]^2 + \text{Im}[h_1^H]^2 \right\}}, \quad (14)$$

with

$$\mathcal{K}(Q) = \sqrt{Q^2(Q^2 - 4m_Z^2)}. \quad (15)$$

Motivated by this result, we propose that a non-zero left-right asymmetry can also arise in the process $Z^* \rightarrow ZH$. For this case, we define \mathcal{A}_{LR}^Z as

$$\mathcal{A}_{LR}^Z = \frac{\Gamma_{Z^* \rightarrow Z_L H}^L - \Gamma_{Z^* \rightarrow Z_R H}^R}{\Gamma_{Z^* \rightarrow Z_L H}^L + \Gamma_{Z^* \rightarrow Z_R H}^R}. \quad (16)$$

To obtain the analytic expression for the \mathcal{A}_{LR}^Z asymmetry, we calculate the polarized width decays $\Gamma_{Z^* \rightarrow Z_\lambda H}^\lambda$ in the following kinematic: the process $Z^*(p_1) \rightarrow Z(p_2)H(q)$ takes place in the rest frame of the $Z^*(p_1)$ boson, with the $Z(p_2)$ moving along the x -axis. In such a scenario, the polarization vectors of the $Z(p_2)$ boson are:

$$\epsilon(0) = \frac{1}{2m_Z P} \left(\sqrt{(P^2 + m_Z^2 - m_H^2)^2 - 4m_Z^2 P^2}, P^2 + m_Z^2 - m_H^2, 0, 0 \right), \quad (17)$$

$$\epsilon(R/L) = \frac{1}{\sqrt{2}} \left(0, 0, -i, \pm 1 \right). \quad (18)$$

We find that the polarized width decays can be expressed as

$$\Gamma_{Z^* \rightarrow Z_\lambda H}^\lambda = \frac{\sqrt{-2m_H^2(m_Z^2 + P^2) + m_H^4 + (m_Z^2 - P^2)^2}}{16\pi P^3} \mathcal{M}^2(\lambda), \quad \lambda = L, R, 0. \quad (19)$$

where λ denotes the polarization of the on-shell Z boson and $\mathcal{M}^2(\lambda)$ is the squared polarized amplitude. We have not averaged over the initial polarizations in Eq (19) because the off-shell $Z(p_1)$ boson corresponds to a propagator in a collider process. The left and right polarized amplitudes are given as

$$\begin{aligned} \mathcal{M}^2(L/R) = & -\frac{g^2}{4c_W^2 m_Z^4} \left\{ m_Z^2 \left[-4m_Z^4 (\text{Re}[h_1^Z]^2 + \text{Im}[h_1^Z]^2) + (\text{Re}[h_3^Z]^2 + \text{Im}[h_3^Z]^2) (2m_H^2(m_Z^2 + P^2) - m_H^4) \right. \right. \\ & \left. \left. - (m_Z^2 - P^2)^2 \right] \mp 4m_Z^4 (\text{Re}[h_1^Z] \text{Im}[h_3^Z] - \text{Im}[h_1^Z] \text{Re}[h_3^Z]) \sqrt{-2m_H^2(m_Z^2 + P^2) + m_H^4 + (m_Z^2 - P^2)^2} \right\}. \end{aligned} \quad (20)$$

Analogous to the $H^* \rightarrow ZZ$ process, the amplitudes for transversely polarized states exhibit a dependence on the h_1^Z and h_3^Z form factors [21]. To ensure a comprehensive analysis, we have computed the amplitude corresponding to longitudinal polarization:

$$\begin{aligned} \mathcal{M}^2(0) = & \frac{g^2}{16c_W^2 m_Z^6} \left\{ 4m_Z^4 \left(\text{Re}[h_1^Z]^2 + \text{Im}[h_1^Z]^2 \right) (-2m_H^2(m_Z^2 + P^2) + m_H^4 - 2P^2 m_Z^2 + 5m_Z^4 + P^4) \right. \\ & + \left[\text{Re}[h_2^Z]^2 + \text{Im}[h_2^Z]^2 \right] [(m_H - m_Z)^2 - P^2] [(m_H + m_Z)^2 - P^2] [m_H^2 - 3m_Z^2 - P^2] [m_H^2 + m_Z^2 - P^2] \\ & \left. + 4m_Z^2 \left(\text{Re}[h_1^Z] \text{Re}[h_2^Z] + \text{Im}[h_1^Z] \text{Im}[h_2^Z] \right) (-m_H^2 + m_Z^2 + P^2) (-2m_H^2(m_Z^2 + P^2) + m_H^4 + (m_Z^2 - P^2)^2) \right\}. \end{aligned} \quad (21)$$

The absence of the CP -violating form factor h_3^Z in this expression suggests that the longitudinal polarization of the Z boson does not provide a significant avenue for probing CP violation. On the other hand, from the last term in Eq. (20), we note a difference in sign between the left- and right-polarized amplitudes, which leads to a non-zero \mathcal{A}_{LR}^Z asymmetry. In terms of the real and imaginary parts of the h_1^Z and h_3^Z form factors, the asymmetry can be expressed as follows

$$\mathcal{A}_{LR}^Z = 4m_Z^2 \mathcal{K}(P) \frac{\text{Im}[h_3^Z] \text{Re}[h_1^Z] - \text{Im}[h_1^Z] \text{Re}[h_3^Z]}{\mathcal{K}^2(P) \left\{ \text{Re}[h_3^Z]^2 + \text{Im}[h_3^Z]^2 \right\} + 4m_Z^4 \left\{ \text{Im}[h_1^Z]^2 + \text{Re}[h_1^Z]^2 \right\}}, \quad (22)$$

where the $\mathcal{K}(P)$ function is given by

$$\mathcal{K}(P) = \sqrt{-2m_H^2(m_Z^2 + P^2) + m_H^4 + (m_Z^2 - P^2)^2}. \quad (23)$$

The \mathcal{A}_{LR}^Z asymmetry exhibits a structure similar to that obtained in the $H^* \rightarrow ZZ$ case. Additionally, we observe that to achieve a non-vanishing \mathcal{A}_{LR}^V ($V = H, Z$), asymmetry, CP -violating and complex anomalous couplings are necessary. In the SM, the h_1^V ($V = H, Z$) form factor is complex [21]. Consequently, having a non-zero h_3^V ($V = H, Z$) would induce the left-right asymmetries discussed in this section.

IV. NUMERICAL ANALYSIS

We will now assess the numerical values of the FCNC contributions to the h_2^V and h_3^V ($V = H, Z$) form factors, as well as the \mathcal{A}_{LR}^V asymmetries. Since we anticipate significant contributions from FCNC couplings involving the top quark, we will consider the bounds outlined in Eqs. (7) and (8). Additionally, our analysis will focus exclusively on energy regions where the ZZ and HZ pairs can be produced on-shell. To numerically evaluate the Passarino-Veltman scalar functions, we utilized the LoopTools package [87].

A. Contributions of Type I

We begin by analyzing the contributions of type I in Fig. 2 for both scenarios: the H^*ZZ and Z^*ZH vertex. To achieve the maximum values for the CP -conserving contributions, we will use the upper bounds on the norm of the g_V^{tc} and g_A^{tc} couplings in Eq. (7). For the CP -violating form factor, it is useful to define

$$\hat{h}_3^V(I) = \frac{h_3^V(I)}{\text{Im}\left[g_V^{ij}g_A^{ij*}\right]}, \quad V = H, Z, \quad (24)$$

to facilitate the analysis of its behavior and contributions in a model-independent manner.

1. H^*ZZ vertex

In Fig. 4, we present the behavior of the real and imaginary parts of $h_2^H(I)$ (left plot) and $\hat{h}_3^H(I)$ (right plot) as a function of Q . For the CP conserving form factor h_2^H , we observe that both parts can reach values up order 10^{-6} , which is four orders of magnitude smaller than those predicted in the SM [21]. The absorptive parts emerge when the particles in the loop that couple to the off-shell boson can be on-shell [88, 89]. Below the threshold energy of $Q = 2m_t$, the imaginary part of h_2^H is approximately of order 10^{-10} . Only the diagrams in Fig 2, where the Higgs couples to charm-anticharm pair, contribute to the imaginary part at these energies. Therefore, $\text{Im}[h_2^H]$ will be extremely small at $Q < 2m_t$. Beyond the threshold energy, additional diagrams involving the $H\bar{t}t$ coupling also contribute. As a result, the imaginary part becomes comparable in magnitude to the real part, and around $Q \approx 500$ GeV, the magnitude of $\text{Im}[h_2^H]$ exceeds that of $\text{Re}[h_2^H]$.

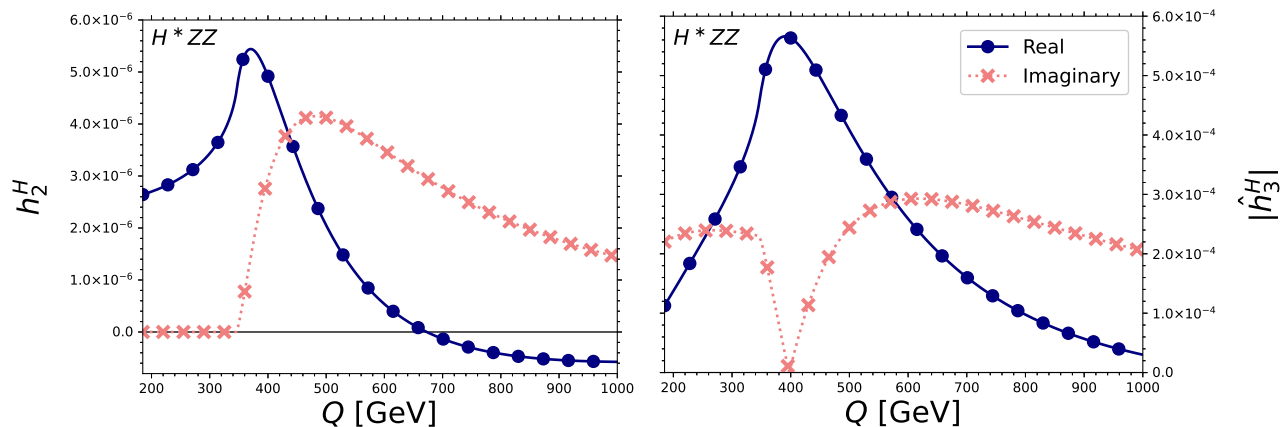


FIG. 4. The FCNC contributions of the Type I to the form factors h_2^H (left plot) and \hat{h}_3^H (right plot) as a function of Q .

For the CP -violating form factor, we find that the contributions to its real and absorptive parts are of order 10^{-4} . Unlike the form factor h_2^H , the imaginary contribution is also relevant for $Q \leq 2m_t$. Furthermore, its magnitude dominates at both low and high energy levels. At energies around 500 GeV, however, the real part is the main

contribution. From the limits in Eq. (7), we estimate that $\text{Im}[g_V g_A^*]$ can reach values of order 10^{-5} . In this context, the real and imaginary parts of h_3^H could achieve magnitudes between 10^{-8} and 10^{-9} . While this result is quite small compared to the current constraints on h_3^H [21], it is three orders of magnitude larger than the SM prediction [22].

2. Z^*ZH

We now show the behavior of $h_2^Z(I)$ (left plot) and $\hat{h}_3^Z(I)$ (right plot) as a function of P , in Fig. 5. For h_2^Z , we observe a pattern similar to the previous case. Both the real and imaginary parts reach magnitudes of order 10^{-6} , with the absorptive part dominating at high energies. However, for values of P less than $2m_t$, the magnitudes of both the imaginary and real parts are comparable, contrasting with the behavior observed for the scenario involving an off-shell Higgs boson. In the case of the Z^*ZH vertex, the amplitudes of the contributing diagrams behave differently, as all exhibit an imaginary component. This phenomenon arises because the $\bar{t}c$ and $\bar{c}t$ pairs, which couple to the Z^* gauge boson in Fig 2, can be on-shell in the energy range $\sqrt{m_H^2 + m_Z^2} < P < 2m_t$. Here $\sqrt{m_H^2 + m_Z^2}$ is the minimum energy required to produce an on-shell HZ pair. Therefore, in the Z^*ZH vertex, the absorptive part is not negligible at low values of P .

For the CP -violating form factor $\hat{h}_3^Z(I)$, both the real and imaginary parts can be as large as those found in the H^*ZZ scenario, although they are significantly smaller as P increases. The imaginary part becomes more relevant in the energy range $300 \text{ GeV} \lesssim P \lesssim 700 \text{ GeV}$. At high values of P , the magnitudes of the real and absorptive parts become similar but of order 10^6 . For $\text{Im}[g_V g_A^*] \sim 10^{-5}$, the magnitude of the form factor h_3^Z can achieve values of order 10^{-8} , which is three orders of magnitude larger than the SM prediction.

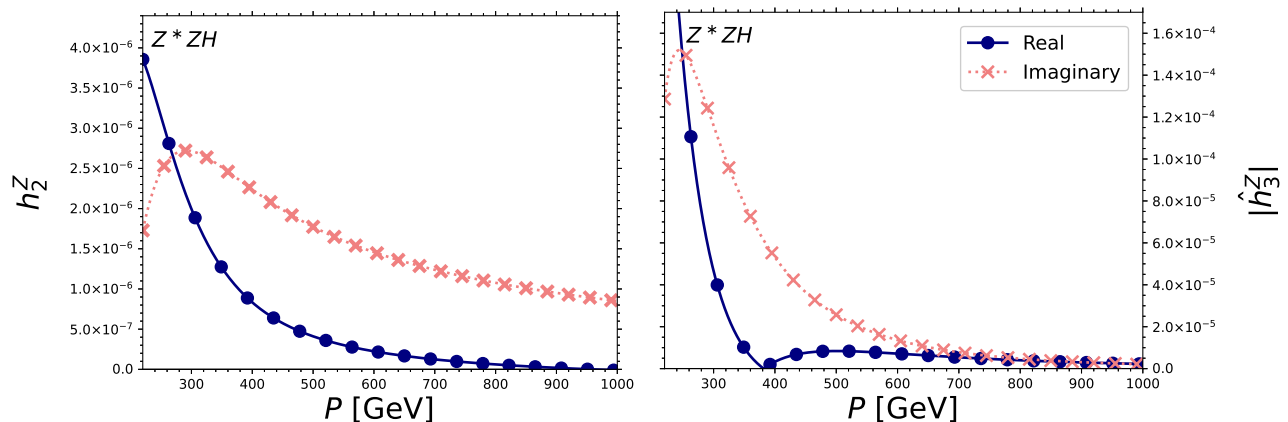


FIG. 5. The FCNC contributions of the type I to the form factors h_2^Z (left plot) and \hat{h}_3^Z (right plot) as a function of P .

B. Contributions of Type II

The form factors obtained from diagrams of type II require a different approach, as they can be expressed through four combinations of the g_r ($r = V, A, S, P$) couplings. To assess the FCNC contributions numerically, we will examine four scenarios that align with the bounds outlined in Eqs. (7) and (8).

- **Scenario I:** As the pseudoscalar coupling in Lagrangian (6) is not essential for inducing CP violation, we focus on the case where $g_P = 0$. We employ the upper limits from Eqs. (7)-(8) to determine the values of the real and imaginary parts of the various combinations involved in the form factors h_2^V and h_3^V . The resulting values are

$$\text{Re}[g_r g_S^*] = 0.0114, \quad r = V, A, \quad (25)$$

$$\text{Im}[g_r g_S^*] = 0.0114, \quad r = V, A. \quad (26)$$

- **Scenario II:** In this scenario, we analyze the impact of negative couplings on the behavior of the form factors. The real and imaginary parts that include the pseudoscalar coupling will be negative. Furthermore, we will

consider the magnitudes of the couplings to be half of the values used in the previous case.

$$\text{Re}[g_r g_S^*] = -\text{Re}[g_r g_P^*] = 0.0057, \quad r = V, A, \quad (27)$$

$$\text{Im}[g_r g_S^*] = -\text{Im}[g_r g_P^*] = 0.0057, \quad r = V, A. \quad (28)$$

- **Scenario III:** Similar to the previous case, but with different negative values of the real and imaginary parts:

$$\text{Re}[g_V g_S^*] = \text{Re}[g_A g_P^*] = -\text{Re}[g_A g_S^*] = -\text{Re}[g_V g_P^*] = 0.0057, \quad (29)$$

$$\text{Im}[g_V g_S^*] = \text{Im}[g_A g_P^*] = -\text{Im}[g_A g_S^*] = -\text{Im}[g_V g_P^*] = 0.0057. \quad (30)$$

- **Scenario IV:** In this scenario, we only consider the contributions from the pseudoscalar coupling ($g_S = 0$). Furthermore, as the CP -violating form factor h_3^V is not vanishing for the case of flavor-conserving couplings, we analyze the contributions to h_3^V that involve only top quarks in the loop. For the h_2^V ($V = H, Z$) form factor, these contributions are of order 10^{-20} and can be neglected. We utilize the same values as those considered in scenario I:

$$\text{Re}[g_r g_P^*] = 0.0114, \quad r = V, A, \quad (31)$$

$$\text{Im}[g_r g_P^*] = 0.0114, \quad r = V, A. \quad (32)$$

1. H^*ZZ

In Fig. 6, we show the behavior of $h_2^H(II)$ as a function of Q for the scenarios $I - III$. At low values of Q in these three scenarios, the dominant contributions correspond to the real part, with the absorptive part being of the same order of magnitude. This behavior contrasts with the observed in the H^*ZZ case, where the imaginary part is only relevant for energies above $2m_t$. As previously mentioned, not all the amplitudes contribute to the imaginary part of h_2^H in the diagrams of type I. However, for all diagrams of type II, the $\bar{t}c$ pair coupled to the Higgs boson in Fig. 3 can be on-shell within the energy range considered. Consequently, their amplitudes contribute to the absorptive part, making the real and imaginary parts comparable for $Q < 2m_t$. At high energies, the imaginary part becomes the largest contribution. The most significant results are obtained in scenarios I and III , yielding values of order 10^{-7} , which are five orders of magnitude smaller than in the SM [21] and one order of magnitude lower than in the H^*ZZ vertex. It is worth noting that although the couplings in scenario III are one order of magnitude smaller than those in scenario I, both cases produce contributions of approximately the same order of magnitude. This finding indicates that contributions from the pseudoscalar coupling can be relevant in FCNC couplings. We do not present scenario IV, which involves only top quarks running in the loop, as h_2^V is of order 10^{-20} . This result suggests that the flavor-conserving contributions associated with the pseudoscalar coupling are small. Additionally, we observe distinct patterns in scenarios II and III , highlighting the significant impact of negative couplings on the behavior of h_2^H .

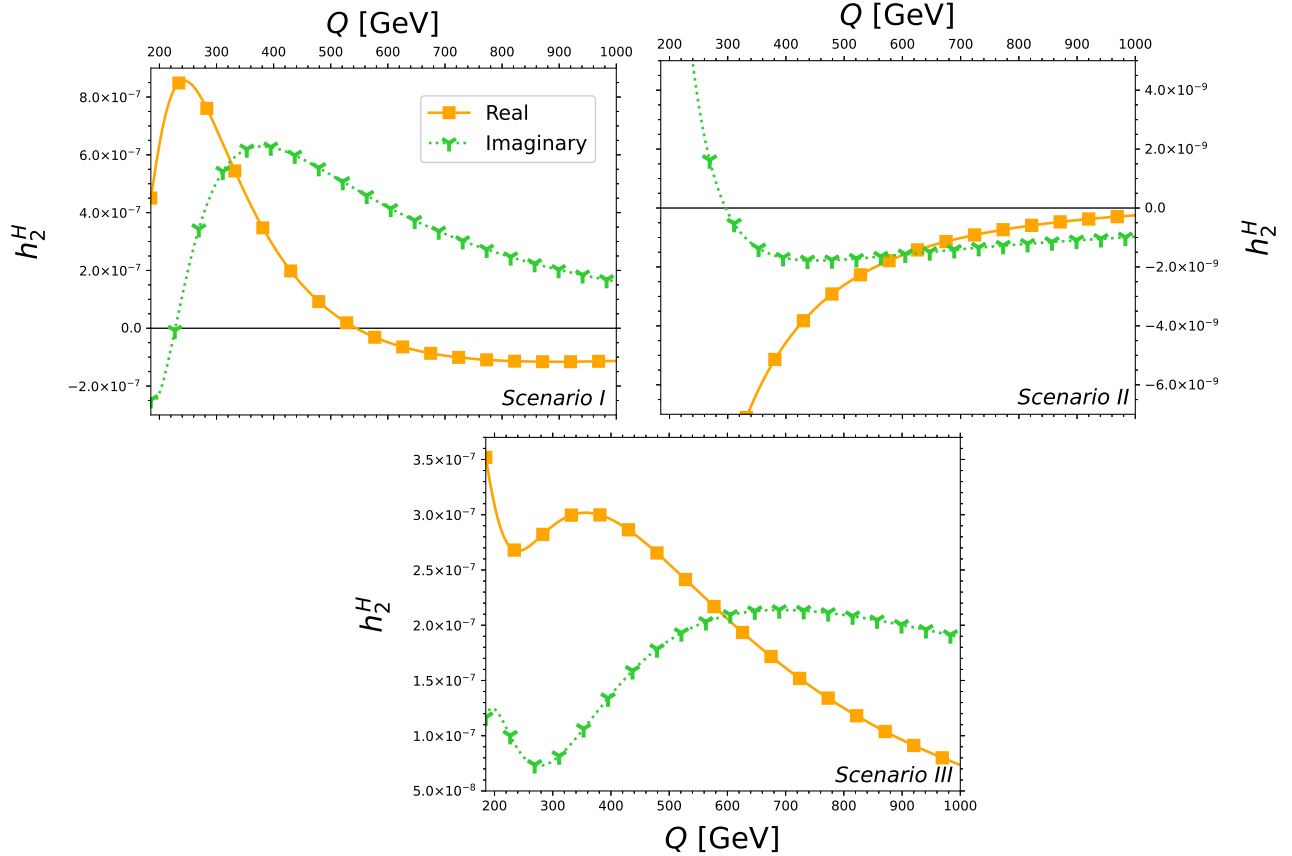


FIG. 6. FCNC contributions of the type II to the h_2^H form factor as a function of Q . For the values of the different couplings, we consider the scenarios *I-III*, whereas the contribution in scenario *IV* is tiny and not shown.

For the CP -violating form factor, we present in Fig. 7 the absolute value of the real and absorptive part of $h_3^H(II)$ as a function of Q . In scenarios *I* and *IV*, the imaginary part dominates nearly the entire energy range. While in scenarios *II* and *III*, it predominates only at lower values of Q . In scenario *IV*, the absorptive part is zero for $Q < 2m_t$, as only top quarks are included in the loop. In the four scenarios, the magnitude of the real and imaginary parts are similar at high energies. The most significant values are observed in scenarios *I* and *IV*, where both the real and imaginary parts can reach magnitudes of order 10^{-6} , which is five orders of magnitude larger than the prediction in the SM [22]. Furthermore, these results are two orders of magnitude larger than those obtained in diagrams of type *I*. Hence, relevant contributions to the left-right asymmetries become feasible. Distinct patterns are evident in the four scenarios, indicating that the values and signs of the couplings play a relevant role in the behavior of h_3^H . In contrast with the CP -conserving form factor h_2^H , the contributions from the pseudoscalar coupling are significant in both flavor-conserving and flavor-violating contexts.

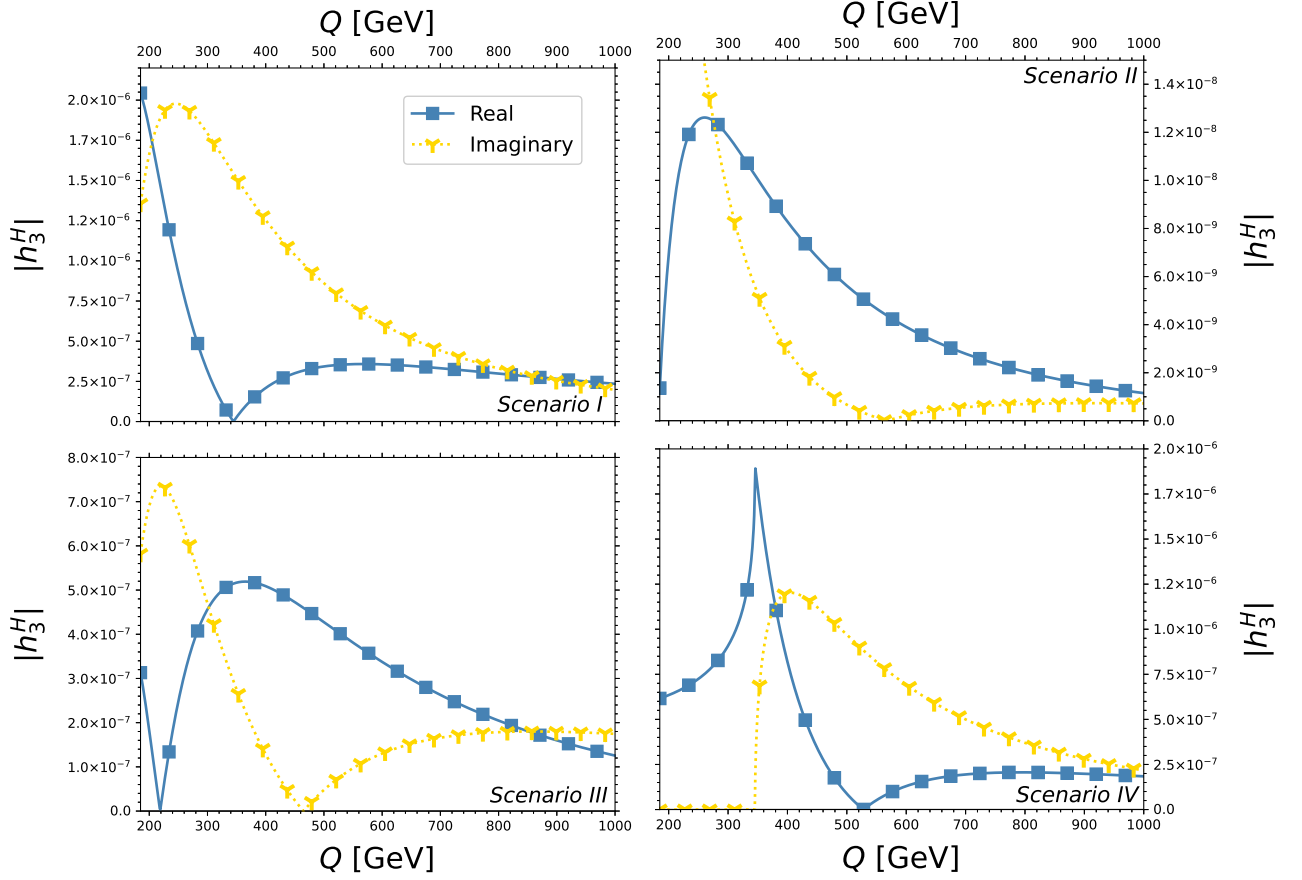


FIG. 7. FCNC contributions of the type II to the h_3^H form factor as a function of Q . For the values of the different couplings, we consider the scenarios *I-IV* discussed in this section.

2. Z^*ZH

For the case of an off-shell Z boson, we present in Fig. 8 the behavior of $h_2^Z(II)$ as a function of Q . In scenarios *I* and *III*, the magnitude of both real and absorptive parts reach the largest values of order 10^{-7} . The real and absorptive contributions dominate in different energy regions in these scenarios. In scenario *II*, the principal contribution corresponds to the imaginary part, which only achieves values around 10^{-8} . Scenario *IV* is not shown, as its contributions are of order 10^{-20} . Similar to the H^*ZZ case, we observe that the sign of the couplings significantly affects the behavior of h_2^Z . Moreover, the pseudoscalar contributions are relevant in the case of flavor-violating couplings. Our results for h_2^Z are similar to those in the case with an off-shell Higgs boson. They are one order of magnitude smaller than those obtained in the diagrams of type *I* and tiny compared with the SM result.

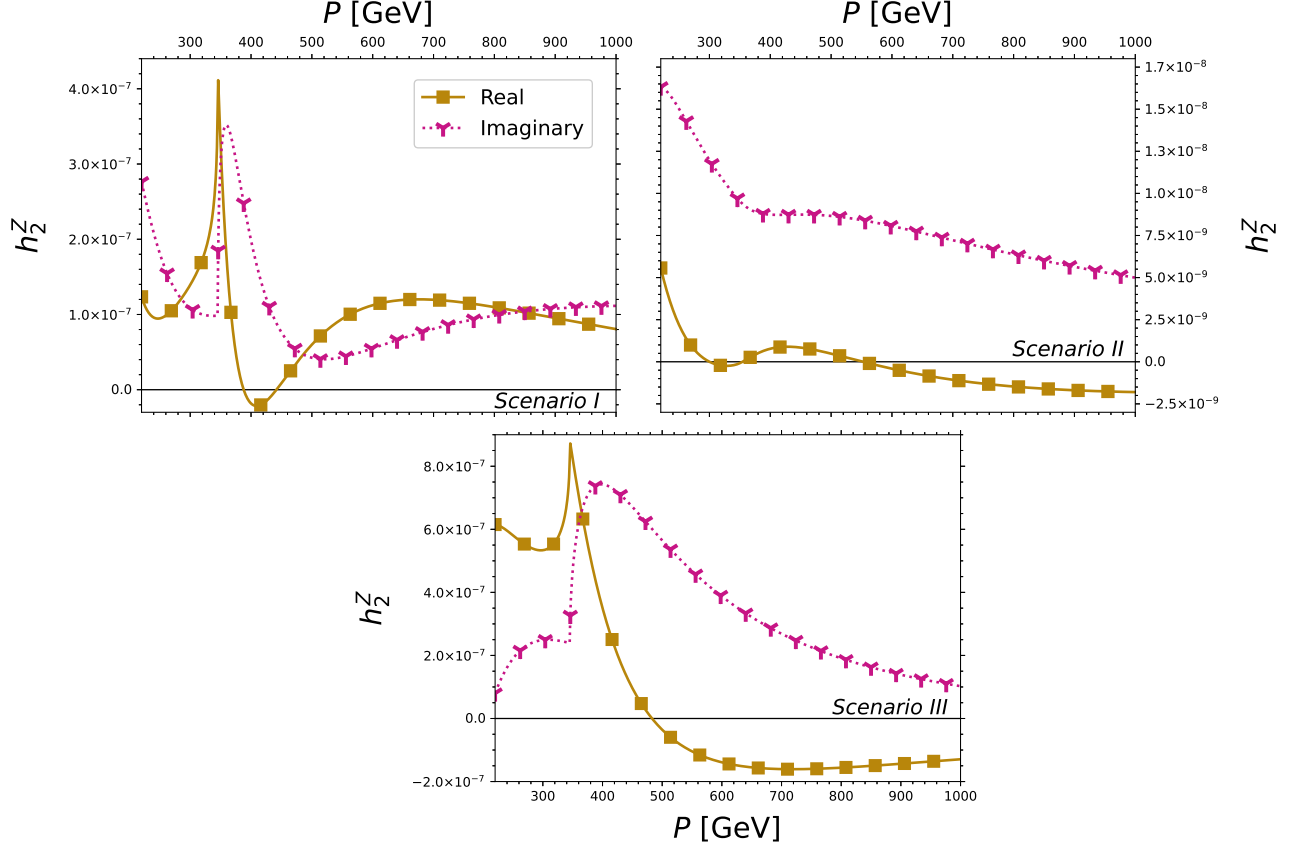


FIG. 8. FCNC contributions of the type II to the h_2^Z form factor as a function of P . For the values of the different couplings, we consider the scenarios *I-III*, whereas the contribution in scenario *IV* is tiny and not shown.

In Fig. 9, we show the absolute value of the real and imaginary parts of the CP -violating form factor $h_3^Z(II)$ for the four scenarios discussed earlier. In scenarios *I – II*, the imaginary part is the dominant contribution for all the values of Q . Conversely, in scenario *III*, the real part is the largest contribution. In scenario *IV*, the absorptive part is zero for energies $Q < 2m_t$ but becomes the main contribution at higher energies. This pattern is reminiscent of the behavior observed in the H^*ZZ case. The magnitudes of the real and absorptive parts of h_3^Z can reach values order 10^{-6} , five and two orders of magnitude larger than the SM and diagrams type *I* predictions, respectively. Additionally, the pseudoscalar coupling plays a relevant role in flavor-conserving and flavor-violating contributions, similar to the observed in the H^*ZZ vertex.

As with the type *I* diagrams, we observe distinct behaviors between h_i^H and h_i^Z ($i = 2, 3$), which do not occur in the SM.

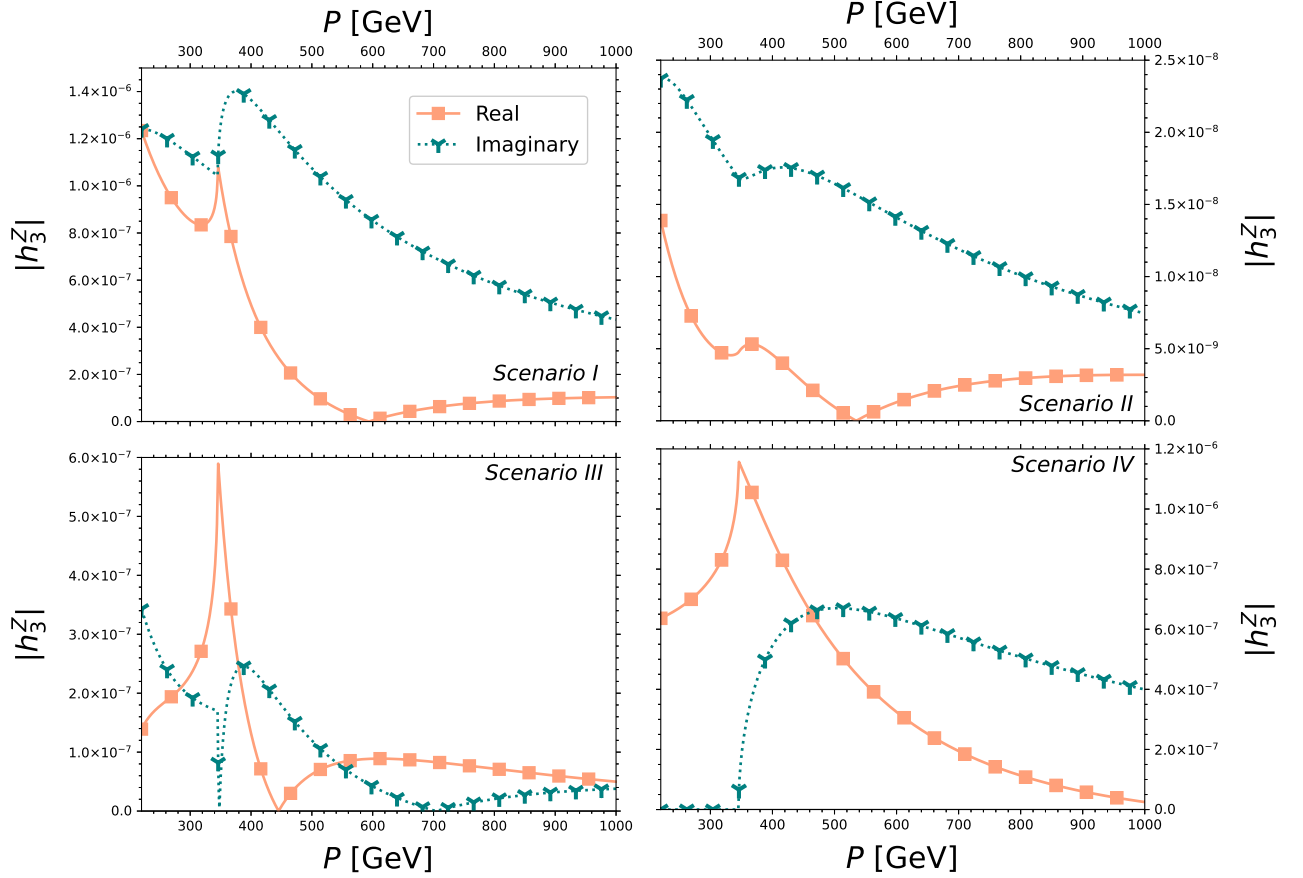


FIG. 9. FCNC contributions of the type II to the h_3^Z form factor as a function of P . For the values of the different couplings, we consider the scenarios *I-IV* discussed in this section.

In summary, the imaginary parts of h_2^V and h_3^V ($V = H, Z$) are comparable to their real parts. This behavior has also been observed in other off-shell couplings, such as trilinear neutral gauge bosons couplings [90, 91] and the $g\bar{q}q$ vertex [92, 93]. The numerical values obtained for the CP -conserving form factor are tiny compared to those predicted in the SM. On the other hand, the contributions to h_3^V can be up to five orders of magnitude larger than in the SM. This form factor and the SM contributions to h_2^V can lead to non-zero left-right asymmetries as discussed in Sec. III. Additionally, we found that new sources of CP violation are possible with a pseudoscalar and without FCNC couplings.

C. Contributions to the \mathcal{A}_{LR}^V ($V = H, Z$) asymmetry

We perform a numerical evaluation of the left-right asymmetries \mathcal{A}_{LR}^V ($V = H, Z$) discussed in Sec. III. The study of the polarizations of the Z bosons has been addressed in various analyses at the LHC [62–67, 71]. Furthermore, several authors have proposed new methods for measuring the polarizations of the ZZ pair in the process $gg \rightarrow H^* \rightarrow ZZ$ [57–61]. Therefore, the \mathcal{A}_{LR}^V ($V = H, Z$) asymmetries may become achievable in the future. The observation of a non-zero asymmetry would indicate the presence of physics beyond the SM.

To study the behavior of the \mathcal{A}_{LR}^V ($V = H, Z$) asymmetries, we note from Eqs. (14) and (22) that only the form factors h_1^V and h_3^V are necessary. For the CP -conserving form factor, we will consider the tree-level and one-loop contributions from the SM. Hence, in Eq. (3), we set $\hat{c}_Z = 0$ and incorporate the one-loop SM results, as reported in Ref. [21], for the anomalous coupling \hat{b}_Z . Regarding the CP -violating form factor h_3^Z , we will utilize the expressions derived from FCNC contributions of both type I and II discussed in Sec. II.

1. Type I

In Fig. 10, we present the \mathcal{A}_{LR}^V ($V = H, Z$) asymmetries as a function of Q and P , considering the FCNC contributions of type I. By using the upper bounds stated in Eq. (7), we find that $\text{Im}[g_V^{tc}g_A^{tc}]$ can reach values of order 10^{-5} . Accordingly, we utilize the values: -8×10^{-5} and 10^{-5} for $\text{Im}[g_V^{tc}g_A^{tc}]$ in Eq. (10). The former value leads to the largest results for both asymmetries, yielding contributions of order 10^{-7} for the case involving an off-shell Higgs and 10^{-8} for the off-shell Z boson. The second value of $\text{Im}[g_V^{tc}g_A^{tc}]$ produces asymmetries that are one order of magnitude smaller. We also observe distinct behaviors between \mathcal{A}_{LR}^H and \mathcal{A}_{LR}^Z , which arise from the different form of the h_1^V form factor in Eq. (3) for the case of an off-shell Higgs or Z boson. Additionally, both asymmetries exhibit an inflection point at $Q = 2m_t$, where the one-loop SM contributions to h_1^V form factors develop a notable imaginary part.

The SM prediction for the CP -violating form factor h_3^H is approximately of order 10^{-11} [22]. Based in this value, the \mathcal{A}_{LR}^H asymmetry has been estimated to be in the range $10^{-8} - 10^{-9}$ [21]. Assuming that h_3^Z is of a similar magnitude to that of an off-shell H boson, we find that \mathcal{A}_{LR}^Z can be of order $10^{-11} - 10^{-12}$ within the SM. Thus, our results in Fig. 10 are one to three orders of magnitude larger than those predicted by the SM when considering type I FCNC contributions.

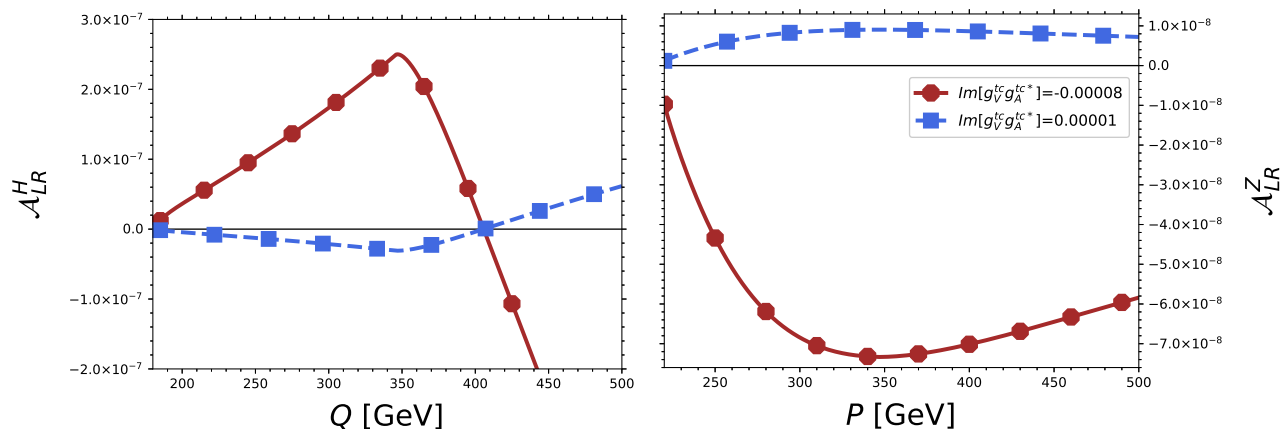


FIG. 10. The asymmetries \mathcal{A}_{LR}^H and \mathcal{A}_{LR}^Z as a function of Q and P , respectively. For the CP -conserving form factor h_2^V ($V = H, Z$), we have considered contributions from the SM up the one-loop level, whereas for h_3^V we used the results obtained for FCNC contributions of type I.

2. Type II

Similar to the previous case, we draw in Fig. 11 the \mathcal{A}_{LR}^V ($V = H, Z$) asymmetries for the contributions of type II. We have examined the four scenarios introduced in Sec. IV B. In both asymmetries, the scenario *II* is negligible, while the remaining scenarios yield values ranging from 10^{-5} to 10^{-6} . The most significant results are obtained in scenarios *I* and *IV*, where h_3^V (*II*) also reaches its highest values.

In scenarios *I* and *III*, we observe that the \mathcal{A}_{LR}^H asymmetry does not exhibit an inflection point at $Q = 2m_t$. This phenomenon can be explained by the absence of any significant change in the imaginary part of the h_3^H at the threshold energy of $2m_t$, as illustrated in Fig. 7. In scenario *IV*, the asymmetries become relevant at $Q = 2m_t$, which aligns with the energy level where the h_1^V and h_3^V ($V = H, Z$) form factors also achieve notable values. These findings indicate that the absorptive parts of the form factors notably influence the behavior of the asymmetries and should be considered in future analyses.

The form factors h_3^V (*II*) can be up to two orders larger than those from the type I diagrams. Consequently, the terms containing the \mathcal{K}^2 functions in the denominator of Eqs. (14) and (22) emerge as the dominant contributions when considering diagrams of type II. Furthermore, since the functions $\mathcal{K}(Q)$ and $\mathcal{K}(P)$ yield nearly identical numerical values, we observe similar patterns between the two asymmetries, contrasting with the results obtained in Fig 10.

Finally, the \mathcal{A}_{LR}^H and \mathcal{A}_{LR}^Z asymmetries in Fig. 11 are two and three orders of magnitude larger than the corresponding from FCNC contributions of type I, respectively. Our results are three to six orders larger than the SM predictions.

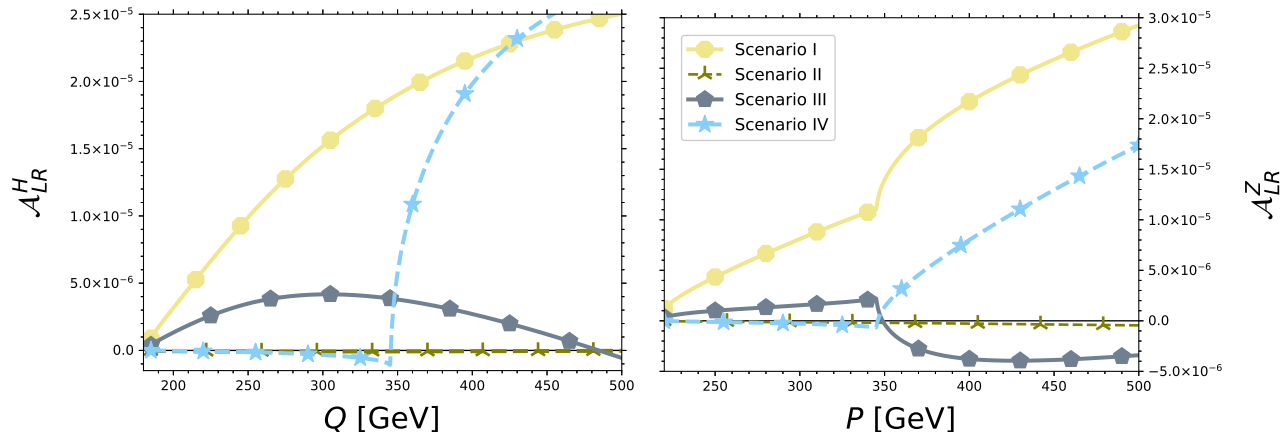


FIG. 11. The asymmetries \mathcal{A}_{LR}^H and \mathcal{A}_{LR}^Z as a function of Q and P , respectively. For the CP -conserving form factor h_2^V ($V = H, Z$), we have considered contributions from the SM up the one-loop level, whereas for h_3^V we used the results obtained for FCNC contributions of type II.

V. CONCLUSIONS

In this work, we have computed new contributions to the H^*ZZ and Z^*ZH vertexes from FCNC couplings mediated by the Z and Higgs bosons. Furthermore, we identified two distinct types of contributing Feynman diagrams. The first contribution, Type I, arises when only the FCNC couplings mediated by the Z boson are considered. When both Z bosons and Higgs FCNC couplings are included, the contribution of Type II emerges. We found new contributions from both scenarios to the form factors h_2^V and h_3^V ($V = H, Z$), with the results expressed in terms of the Passarino-Veltman scalar functions. Notably, the CP -violating form factor h_3^V can be induced without flavor violation in a pseudoscalar coupling scenario. Using bounds on the FCNC couplings of the top quark, we determined that the contributions to h_2^V can be of order $10^{-6} - 10^{-7}$, significantly small compared with those in the SM. In contrast, the CP -violating form factor can reach values of 10^{-8} and 10^{-6} for Type I and Type II contributions, respectively. These estimates are three and five orders of magnitude larger than the predictions of the SM. We also find that the absorptive part is comparable to the real part and is the dominant contribution in some energy regions.

We have also calculated the \mathcal{A}_{LR}^Z asymmetry for the $Z^* \rightarrow ZH$ process. Our results show that the \mathcal{A}_{LR}^Z has a similar form to the reported for the $H^* \rightarrow ZZ$ case, as both are in terms of the form factors h_1^V and h_3^V . Using the SM one-loop level expressions for h_1^V along with the contributions from FCNC couplings to h_3^V , we find that \mathcal{A}_{LR}^H and \mathcal{A}_{LR}^Z can reach significantly larger values than those derived from SM contributions alone. The most significant results arise from contributions of Type II, where the asymmetries can be up to six orders of magnitude larger than in the SM. Additionally, we observe that the imaginary parts of the form factors considerably influence the behavior of the asymmetries. This finding suggests that the absorptive parts can not be ignored when studying physical observables. The observation of a non-zero left-right asymmetry \mathcal{A}_{LR}^V ($V = H, Z$) would imply the existence of CP violation in the HZZ vertex.

ACKNOWLEDGMENTS

This work was supported by UNAM Posdoctoral Program (POSDOC) and PAPIIT project IN105825 "Estudios de física del sabor y violación de CP en modelos de nueva física". We also acknowledge support from Sistema Nacional de Investigadores (Mexico).

Appendix A: Analytical Forms

This appendix presents the analytical expressions for the functions appearing in the h_2^V and h_3^V ($V = H, Z$) form factors. Our results are in terms of the Passarino-Veltman scalar functions. We introduce the shorthand notation:

$$B_{ij}(c^2) = B_0(c^2, m_i^2, m_j^2), \quad (\text{A1})$$

$$C_{ijk}(Q^2) = C_0(m_Z^2, m_Z^2, Q^2, m_i^2, m_j^2, m_k^2), \quad (\text{A2})$$

$$C_{ijk}(P^2) = C_0(m_H^2, m_Z^2, P^2, m_i^2, m_j^2, m_k^2), \quad (\text{A3})$$

where B_0 and C_0 are the usual two- and three-point Passarino-Veltman scalar functions. The following symmetry relations will also be useful

$$B_{ij}(c^2) = B_{ji}(c^2), \quad (\text{A4})$$

$$C_{ijk}(c^2) = C_{kji}(c^2). \quad (\text{A5})$$

1. Diagrams type I

The functions A_V^V and A_A^V ($V = H, Z$) for contributions of Type I are given as follows:

$$\begin{aligned}
A_V^H(Q^2, m_i^2, m_j^2) = & \frac{1}{Q^2(Q^2 - 4m_Z^2)^2} \left\{ \left[4m_i^2(m_i^2 - m_j^2)(4m_Z^2 - Q^2) \right] B_{ii}(0) + \left[4m_j^2(m_j^2 - m_i^2)(4m_Z^2 - Q^2) \right] B_{jj}(0) \right. \\
& + \left[2Q^4(m_i - m_j)^2 - 4Q^2\{m_Z^2(-4m_i m_j + m_i^2 + m_j^2) + (m_i^2 - m_j^2)^2\} \right. \\
& + \left. 8m_Z^4(m_i^2 + m_j^2) - 8m_Z^2(m_i^2 - m_j^2)^2 \right] B_{ij}(m_Z^2) + 2m_i \left[Q^4(m_j - m_i) \right. \\
& + \left. 2Q^2\{m_Z^2(m_i - 2m_j) + 2m_i(m_i - m_j)(m_i + m_j)\} - 4m_i m_Z^2(m_i^2 - m_j^2 + m_Z^2) \right] B_{ii}(Q^2) \\
& + 2m_j \left[Q^4(m_i - m_j) + 2Q^2\{m_Z^2(m_j - 2m_i) + 2m_j(m_j - m_i)(m_j + m_i)\} \right. \\
& - \left. 4m_j m_Z^2(m_j^2 - m_i^2 + m_Z^2) \right] B_{jj}(Q^2) + m_i \left[2Q^4\{-m_Z^2(m_i + 3m_j) - m_i^2 m_j - 3m_i m_j^2 \right. \\
& + \left. m_i^3 + m_j^3\} + 8Q^2\{m_Z^2(m_i^2 m_j + 2m_i m_j^2 + m_i^3 - m_j^3) - m_i(m_i^2 - m_j^2)^2 + m_j m_Z^4\} \right. \\
& + \left. 8m_i m_Z^2(m_i - m_j - m_Z)(m_i + m_j - m_Z)(m_i - m_j + m_Z)(m_i + m_j + m_Z) + Q^6 m_j \right] C_{iji}(Q^2) \\
& + m_j \left[2Q^4\{-m_Z^2(m_j + 3m_i) - m_j^2 m_i - 3m_j m_i^2 + m_j^3 + m_i^3\} + 8Q^2\{m_Z^2(m_j^2 m_i + 2m_j m_i^2 \right. \\
& + \left. m_j^3 - m_i^3) - m_j(m_j^2 - m_i^2)^2 + m_i m_Z^4\} + 8m_j m_Z^2(m_j - m_i - m_Z)(m_j + m_i - m_Z) \right. \\
& \times \left. (m_j - m_i + m_Z)(m_j + m_i + m_Z) + Q^6 m_i \right] C_{jij}(Q^2) \\
& \left. + 2 \left[4m_Z^2 - Q^2 \right] \left[m_i^2(-4m_j^2 - 2m_Z^2 + Q^2) + 2m_i^4 + m_j^2(2m_j^2 - 2m_Z^2 + Q^2) \right] \right\} \quad (\text{A6})
\end{aligned}$$

$$\begin{aligned}
A_A^H(Q^2, m_i^2, m_j^2) = & A_V^H(Q^2, m_i^2, m_j^2) - \frac{1}{Q^2(Q^2 - 4m_Z^2)^2} 2Q^2 m_i m_j (Q^2 - 4m_Z^2) \left[-4B_{ij}(m_Z^2) + 2B_{ii}(Q^2) + 2B_{jj}(Q^2) \right. \\
& \left. + \{Q^2 - 2(m_i^2 - m_j^2 + m_Z^2)\} C_{ij}(Q^2) + \{2m_i^2 - 2(m_j^2 + m_Z^2) + Q^2\} C_{ji}(Q^2) \right] \quad (\text{A7})
\end{aligned}$$

$$\begin{aligned}
A_V^Z(P^2, m_i^2, m_j^2) = & \frac{1}{((m_H - m_Z)^2 - P^2)((m_H + m_Z)^2 - P^2)} \left\{ -4m_i^2 (m_i - m_j) (m_i + m_j) B_{ii}(0) \right. \\
& + m_i \left[\frac{3m_H m_i (m_Z (m_H + m_Z) + m_i^2 - m_j^2)}{m_H + m_Z - P} + \frac{3m_H m_i (m_Z (m_Z - m_H) + m_i^2 - m_j^2)}{m_H - m_Z + P} \right. \\
& - \frac{3m_H m_i (m_Z (m_Z - m_H) + m_i^2 - m_j^2)}{-m_H + m_Z + P} + \left. \frac{3m_H m_i (m_Z (m_H + m_Z) + m_i^2 - m_j^2)}{m_H + m_Z + P} \right. \\
& - 2 (m_i (m_H^2 - 2m_j^2 + m_Z^2) - m_H^2 m_j + 2m_i^3) - 2P^2 m_i \left. \right] B_{ii}(m_H^2) \\
& + \left[\frac{3m_Z (-m_H m_Z (m_i^2 + m_j^2) + m_Z^2 (m_i^2 + m_j^2) + (m_i^2 - m_j^2)^2)}{-m_H + m_Z - P} \right. \\
& + \frac{3m_Z (m_i^2 (m_Z (m_H + m_Z) - 2m_j^2) + m_j^2 (m_Z (m_H + m_Z) + m_j^2) + m_i^4)}{m_H + m_Z - P} \\
& + \frac{3m_Z (-m_H m_Z (m_i^2 + m_j^2) + m_Z^2 (m_i^2 + m_j^2) + (m_i^2 - m_j^2)^2)}{-m_H + m_Z + P} \\
& + \frac{3m_Z (m_i^2 (m_Z (m_H + m_Z) - 2m_j^2) + m_j^2 (m_Z (m_H + m_Z) + m_j^2) + m_i^4)}{m_H + m_Z + P} - 2m_H^2 m_i m_j \\
& + m_H^2 m_i^2 + m_H^2 m_j^2 - P^2 (m_i - m_j)^2 - 2m_i m_j m_Z^2 + 4m_i^2 m_j^2 - 9m_i^2 m_Z^2 - 2m_i^4 - 9m_j^2 m_Z^2 \\
& - 2m_j^4 \left. \right] \frac{B_{ij}(m_Z^2)}{2} + \frac{1}{((m_H - m_Z)^2 + P^2)((m_H + m_Z)^2 - P^2)} \left[-2m_i m_j ((m_H - m_Z)^2 - P^2) \right. \\
& \times ((m_H + m_Z)^2 - P^2) (m_H^2 - m_Z^2 + P^2) + m_i^2 (-5P^4 (m_H^2 + 4m_j^2 - m_Z^2) \\
& + P^2 (16m_j^2 (m_H^2 + m_Z^2) + 6m_H^2 m_Z^2 + m_H^4 - 7m_Z^4) + (m_H^2 - m_Z^2)^2 (m_H^2 + 4m_j^2 - m_Z^2) + 3P^6) \\
& - 2m_i^4 (4P^2 (m_H^2 + m_Z^2) + (m_H^2 - m_Z^2)^2 - 5P^4) + m_j^2 (5P^4 (-m_H^2 + 2m_j^2 + m_Z^2) \\
& + P^2 (-8m_j^2 (m_H^2 + m_Z^2) + 6m_H^2 m_Z^2 + m_H^4 - 7m_Z^4) + (m_H^2 - m_Z^2)^2 (m_H^2 - 2m_j^2 - m_Z^2) \\
& + 3P^6) \left. \right] \frac{B_{ij}(P^2)}{2} + \frac{m_i}{((m_H - m_Z)^2 - P^2)((m_H + m_Z)^2 - P^2)} \left[2m_i^3 (m_j^2 (-4m_H^2 (m_Z^2 + P^2) \right. \\
& + 8m_H^4 - 4(m_Z^2 - P^2)^2) + 2m_H^4 (m_Z^2 + P^2) + m_H^2 (6P^2 m_Z^2 - 7m_H^4 - 7P^4) + m_H^6 \\
& + 4(m_Z^2 - P^2)^2 (m_Z^2 + P^2)) + m_i (4m_j^4 (m_H^2 (m_Z^2 + P^2) - 2m_H^4 + (m_Z^2 - P^2)^2) \\
& + 2m_j^2 (4m_H^4 (m_Z^2 + P^2) + m_H^2 (-10P^2 m_Z^2 + m_Z^4 + P^4) - 3m_H^6 - 2(m_Z^2 - P^2)^2 (m_Z^2 + P^2)) \\
& + (-m_H^2 + m_Z^2 + P^2) (-P^4 (2m_H^2 + m_Z^2) + P^2 (8m_H^2 m_Z^2 + m_H^4 - m_Z^4) + (m_Z^3 - m_H^2 m_Z)^2 \\
& + P^6) - 2m_H^2 m_i^2 m_j ((m_H - m_Z)^2 - P^2) ((m_H + m_Z)^2 - P^2) + 4m_i^5 (m_H^2 (m_Z^2 + P^2) \\
& - 2m_H^4 + (m_Z^2 - P^2)^2) + m_H^2 m_j ((m_H - m_Z)^2 - P^2) ((m_H + m_Z)^2 - P^2) (m_H^2 + 2m_j^2 - m_Z^2 \\
& - P^2) \left. \right] C_{ij}(P^2) + (m_i^2 (-m_H^2 + 4m_j^2 + m_Z^2 + P^2) + m_j^2 (-m_H^2 - 2m_j^2 + m_Z^2 + P^2) - 2m_i^4) \\
& + (i \leftrightarrow j) \left. \right\}. \tag{A8}
\end{aligned}$$

$$\begin{aligned}
A_A^Z(p^2, m_i^2, m_j^2) = & A_V^Z(P^2, m_i^2, m_j^2) - \frac{2m_i m_j}{((m_H - m_Z)^2 - P^2)((m_H + m_Z)^2 - P^2)} \left[-2m_H^2 \{ B_{ij}(P^2) + B_{ij}(m_Z^2) \} \right. \\
& + 2m_H^2 \{ B_{ii}(m_H^2) + B_{jj}(m_H^2) \} + 2P^2 \{ B_{ij}(m_Z^2) - B_{ij}(P^2) \} + 2m_Z^2 \{ B_{ij}(P^2) - B_{ij}(m_Z^2) \} \\
& + m_H^2 (m_H^2 - 2m_i^2 + 2m_j^2 - m_Z^2 - P^2) C_{ij}(P^2) + m_H^2 (m_H^2 + 2m_i^2 - 2m_j^2 - m_Z^2 - P^2) C_{jji}(P^2) \left. \right] \tag{A9}
\end{aligned}$$

The functions $\tilde{\mathcal{F}}^V$ ($V = H, Z$) for contributions of Type I are expressed as follows:

$$\begin{aligned} \tilde{\mathcal{F}}^H(Q^2, m_i, m_j) = & \frac{1}{(4m_Z^2 - Q^2)} \left\{ 2[B_{jj}(Q^2) - B_{ii}(Q^2)] + [2(m_i^2 - m_j^2 + m_Z^2) - Q^2]C_{iji}(Q^2) \right. \\ & \left. + [2(m_i^2 - m_j^2 - m_Z^2) + Q^2]C_{jij}(Q^2) \right\}, \end{aligned} \quad (\text{A10})$$

$$\begin{aligned} \tilde{\mathcal{F}}^Z(Q^2, m_i, m_j) = & - \frac{m_H^2}{((m_H - m_Z)^2 - P^2)((m_H + m_Z)^2 - P^2)} \left\{ 2[B_{jj}(m_H^2) - B_{ii}(m_H^2)] \right. \\ & \left. + (-m_H^2 + 2m_i^2 - 2m_j^2 + m_Z^2 + P^2)C_{ijj}(P^2) + (m_H^2 + 2m_i^2 - 2m_j^2 - m_Z^2 - P^2)C_{jji}(P^2) \right\} \end{aligned} \quad (\text{A11})$$

2. Diagrams type II

The functions $R_{1,2,3,4}^V$ ($V = H, Z$) for contributions of Type II are given as follows:

$$\begin{aligned} R_1^H(Q^2, m_i, m_j) = & \frac{1}{Q^4(Q^2 - 4m_Z^2)^2} \left\{ m_Z^2 [6m_i^2 m_j (Q^2 - 2m_Z^2) - m_i (6m_j^2 (Q^2 - 2m_Z^2) - 10Q^2 m_Z^2 + Q^4) \right. \\ & + 6m_i^3 (Q^2 - 2m_Z^2) + 3m_j (Q^2 - 2m_j^2) (Q^2 - 2m_Z^2)] B_{ii}(m_Z^2) \\ & + Q^2 m_Z^2 (m_i + m_j) (2m_Z^2 + Q^2) [B_{ij}(m_Z^2) - 2B_{ij}(Q^2)] \\ & + [-6m_i^4 m_j m_Z^2 (Q^2 - 2m_Z^2) - 2m_i^3 (Q^6 - m_Z^2 (6m_j^2 + 5Q^2) (Q^2 - 2m_Z^2)) \\ & - 2m_i^2 m_j (Q^2 - 2m_Z^2) (Q^4 - m_Z^2 (6m_j^2 + Q^2)) + m_i (4m_Z^4 (Q^2 m_j^2 + 3m_j^4 + 2Q^4) \\ & + m_Z^2 (2Q^4 m_j^2 - 6Q^2 m_j^4 - 7Q^6) + 4Q^2 m_Z^6 + Q^8) - 6m_i^5 m_Z^2 (Q^2 - 2m_Z^2) \\ & + m_j m_Z^2 (2m_Z^2 - Q^2) (-6Q^2 m_j^2 + 6m_j^4 + 2Q^2 m_Z^2 + Q^4)] C_{ijj}(Q^2) \\ & \left. - Q^2 (m_i + m_j) (-6Q^2 m_Z^2 + 8m_Z^4 + Q^4) \right\} + (i \leftrightarrow j), \end{aligned} \quad (\text{A12})$$

$$\begin{aligned} R_2^H(Q^2, m_i, m_j) = & \frac{1}{Q^4(Q^2 - 4m_Z^2)^2} \left\{ (Q^2 - 2m_Z^2) (m_Z^2 (-m_i (6m_j^2 + 5Q^2) - 6m_i^2 m_j + 6m_i^3 - 3Q^2 m_j + 6m_j^3) \right. \\ & + 2Q^4 m_i) B_{ii}(m_Z^2) + Q^2 (m_i - m_j) (-3Q^2 m_Z^2 + 2m_Z^4 + Q^4) [B_{ij}(m_Z^2) - 2B_{ij}(Q^2)] \\ & - (Q^2 - 2m_Z^2) (2Q^2 m_Z^4 (m_i - m_j) + m_Z^2 (2m_i m_j^2 (Q^2 - 6m_i^2) + 6m_j^3 (2m_i^2 + Q^2) \\ & - m_j (-2Q^2 m_i^2 + 6m_i^4 + Q^4) + 6m_i m_j^4 - 3Q^4 m_i - 10Q^2 m_i^3 + 6m_i^5 - 6m_j^5) \\ & + Q^4 m_i (2(m_i - m_j) (2m_i + m_j) + Q^2) C_{ijj}(Q^2) \\ & \left. - Q^2 (m_i - m_j) (-6Q^2 m_Z^2 + 8m_Z^4 + Q^4) \right\} - (i \leftrightarrow j), \end{aligned} \quad (\text{A13})$$

$$\begin{aligned}
R_3^H(Q^2, m_i, m_j) = & \frac{1}{Q^4(Q^2 - 4m_Z^2)^2} \left\{ (Q^2 - 2m_Z^2) (m_Z^2 (-m_i (6m_j^2 + 5Q^2) + 6m_i^2 m_j + 6m_i^3 + 3m_j (Q^2 - 2m_j^2))) \right. \\
& + 2Q^4 m_i B_{ii}(m_Z^2) + Q^2 (m_i + m_j) (-3Q^2 m_Z^2 + 2m_Z^4 + Q^4) [B_{ij}(m_Z^2) - 2B_{ij}(Q^2)] \\
& - (Q^2 - 2m_Z^2) (2Q^2 m_Z^4 (m_i + m_j) + m_Z^2 (2m_i m_j^2 (Q^2 - 6m_i^2) - 6m_j^3 (2m_i^2 + Q^2) \\
& + m_j (-2Q^2 m_i^2 + 6m_i^4 + Q^4) + 6m_i m_j^4 - 3Q^4 m_i - 10Q^2 m_i^3 + 6m_i^5 + 6m_j^5) \\
& + Q^4 m_i (2(2m_i - m_j)(m_i + m_j) + Q^2) C_{ij}(Q^2) \\
& \left. - Q^2 g_A (m_i + m_j) (-6Q^2 m_Z^2 + 8m_Z^4 + Q^4) \right\} + (i \leftrightarrow j), \tag{A14}
\end{aligned}$$

$$\begin{aligned}
R_4^H(Q^2, m_i, m_j) = & \frac{1}{Q^4(Q^2 - 4m_Z^2)^2} \left\{ m_Z^2 (-6m_i^2 m_j (Q^2 - 2m_Z^2) - m_i (6m_j^2 (Q^2 - 2m_Z^2) - 10Q^2 m_Z^2 + Q^4) \right. \\
& + 6m_i^3 (Q^2 - 2m_Z^2) - 3m_j (Q^2 - 2m_j^2) (Q^2 - 2m_Z^2)) B_{ii}(m_Z^2) \\
& + Q^2 g_V m_Z^2 (m_i - m_j) (2m_Z^2 + Q^2) [B_{ij}(m_Z^2) - 2B_{ij}(Q^2)] \\
& + (6m_i^4 m_j m_Z^2 (Q^2 - 2m_Z^2) - 2m_i^3 (Q^6 - m_Z^2 (6m_j^2 + 5Q^2) (Q^2 - 2m_Z^2)) \\
& + 2m_i^2 m_j (Q^2 - 2m_Z^2) (Q^4 - m_Z^2 (6m_j^2 + Q^2)) + m_i (4m_Z^4 (Q^2 m_j^2 + 3m_j^4 + 2Q^4) \\
& + m_Z^2 (2Q^4 m_j^2 - 6Q^2 m_j^4 - 7Q^6) + 4Q^2 m_Z^6 + Q^8) - 6m_i^5 m_Z^2 (Q^2 - 2m_Z^2) \\
& + m_j m_Z^2 (Q^2 - 2m_Z^2) (-6Q^2 m_j^2 + 6m_j^4 + 2Q^2 m_Z^2 + Q^4) C_{ij}(Q^2) \\
& \left. - Q^2 (m_i - m_j) (-6Q^2 m_Z^2 + 8m_Z^4 + Q^4) \right\} - (i \leftrightarrow j), \tag{A15}
\end{aligned}$$

$$\begin{aligned}
R_1^Z(Q^2, m_i, m_j) = & \frac{1}{((m_Z + m_H)^2 - P^2)^2 ((m_Z - m_H)^2 - P^2)^2} \left\{ \frac{P^2}{2} \left[2m_Z^2 (m_i (4(m_H^2 + P^2) + 3m_j^2) \right. \right. \\
& - 3m_i^2 m_j - 3m_i^3 + 3m_j^3) - (P^2 - m_H^2) (m_i (-m_H^2 - 6m_j^2 + P^2) - 3m_j (-m_H^2 + 2m_j^2 + P^2) \\
& + 6m_i^2 m_j + 6m_i^3) + m_Z^4 (- (7m_i + 3m_j)) \left. \right] B_{ii}(P^2) + \frac{m_Z^2}{2} \left[2m_Z^2 (- 3m_j (m_H^2 + m_i^2) \right. \\
& + m_i (m_H^2 - 3m_i^2 + 4P^2) + 3m_i m_j^2 + 3m_j^3) - (P^2 - m_H^2) (m_i (-m_H^2 - 6m_j^2 + 7P^2) \\
& + 3m_j (m_H^2 - 2m_j^2 + P^2) + 6m_i^2 m_j + 6m_i^3) + m_Z^4 (- (m_i - 3m_j)) \left. \right] B_{ii}(m_Z^2) \\
& + \frac{P^2}{2} (m_i + m_j) (4m_Z^2 (m_H^2 + P^2) + (P^2 - m_H^2)^2 - 5m_Z^4) B_{ij}(P^2) \\
& + \frac{m_Z^2}{2} (m_i + m_j) (m_H^2 (4P^2 - 2m_Z^2) + m_H^4 + 4P^2 m_Z^2 + m_Z^4 - 5P^4) B_{ij}(m_Z^2) \\
& - (m_i + m_j) (m_H^4 (m_Z^2 + P^2) - 2m_H^2 (-4P^2 m_Z^2 + m_Z^4 + P^4) + (P^2 - m_Z^2)^2 (m_Z^2 + P^2)) B_{ij}(m_H^2) \\
& + \frac{1}{4} \left[- m_H^6 (2m_i^2 m_j + m_i (4m_Z^2 + 3P^2) + 2m_i^3 + P^2 m_j) + m_H^4 (m_Z^2 (6m_i^2 m_j - P^2 m_i + 6m_i^3 \right. \\
& - 3P^2 m_j) + P^2 (m_i + m_j) (-4m_i m_j + 4m_i^2 + 6m_j^2 + 3P^2) + 6m_i m_Z^4) \\
& + m_H^2 (m_Z^4 (-6m_i^2 m_j + 5P^2 m_i - 6m_i^3 + 3P^2 m_j) + 4P^2 m_Z^2 (m_i + m_j) (2m_i m_j - 3m_i^2 + P^2) \\
& - P^2 (2m_i^3 (P^2 - 6m_j^2) - 6m_i^2 m_j (2m_j^2 + P^2) + m_i (4P^2 m_j^2 + 6m_j^4 + P^4) + 6m_i^4 m_j + 6m_i^5 \\
& + 3m_j (4P^2 m_j^2 + 2m_j^4 + P^4)) - 4m_i m_Z^6) + m_H^8 m_i + m_Z^6 (2m_i^2 m_j - P^2 m_i + 2m_i^3 + P^2 m_j) \\
& - P^2 m_Z^4 (m_i + m_j) (4m_i m_j - 8m_i^2 + 6m_j^2 + P^2) + P^2 m_Z^2 (- 2m_i^3 (6m_j^2 + 5P^2) \\
& - 2m_i^2 m_j (6m_j^2 + P^2) + m_i (8P^2 m_j^2 + 6m_j^4 + P^4) + 6m_i^4 m_j + 6m_i^5 - P^4 m_j + 6m_j^5) \\
& + P^4 (2 (m_i + m_j) (-2P^2 m_i m_j + 3m_j^2 (P^2 - 2m_i^2) + 3m_i^4 + 3m_j^4) + P^4 m_j) + m_i m_Z^8 \left. \right] C_{iji}(P^2) \\
& + \frac{1}{4} \left[m_Z^6 (- m_j (3m_H^2 + 4m_i^2 + P^2) + m_i (P^2 - m_H^2) + 2m_i m_j^2 + 6m_j^3) \right. \\
& + m_i (P^2 - m_H^2)^3 (-m_H^2 + 2m_i (m_i + m_j) + P^2) + m_Z^4 (m_i + m_j) (2m_H^2 (4m_i m_j - m_i^2 \\
& - 6m_j^2 + 2P^2) + 3m_H^4 + 8P^2 m_i m_j - 2m_i^2 (6m_j^2 + 5P^2) + 6m_i^4 + 6m_j^4 - P^4) \\
& - m_Z^2 (P^2 - m_H^2) (6m_j^3 (m_H^2 + 2m_i^2 + P^2) + 2m_i m_j^2 (m_H^2 + 6m_i^2 + 5P^2) - m_j (4P^2 m_H^2 \\
& + m_H^4 + 4P^2 m_i^2 + 6m_i^4 + P^4) + m_i (4m_H^2 (m_i^2 - P^2) - 3m_H^4 - 8P^2 m_i^2 - 6m_i^4 + P^4) - 6m_i m_j^4 \\
& \left. - 6m_j^5) + m_j m_Z^8 \right] C_{jii}(P^2) \\
& + (m_i + m_j) ((m_H - m_Z)^2 - P^2) ((m_H + m_Z)^2 - P^2) (-m_H^2 + m_Z^2 + P^2) \left. \right\} + (i \leftrightarrow j) \quad (A16)
\end{aligned}$$

$$\begin{aligned}
R_2^Z(Q^2, m_i, m_j) = & \frac{1}{((m_Z + m_H)^2 - P^2)^2 ((m_Z - m_H)^2 - P^2)^2} \left\{ \frac{1}{2} (-m_H^2 + m_Z^2 + P^2) (m_i (m_H^2 (4m_Z^2 + P^2) \right. \\
& - 2m_H^4 + 6P^2 m_j^2 + P^2 m_Z^2 - 2m_Z^4 + P^4) + 3P^2 m_j (m_H^2 - 2m_j^2 + m_Z^2 - P^2) + 6P^2 m_i^2 m_j \\
& - 6P^2 m_i^3) B_{ii}(P^2) - \frac{1}{2} (-m_H^2 + m_Z^2 + P^2) (-m_Z^2 (m_i (m_H^2 + 6m_j^2 + P^2) + 3m_j (m_H^2 - 2m_j^2 \\
& + P^2) + 6m_i^2 m_j - 6m_i^3) + 2m_i (P^2 - m_H^2)^2 + m_Z^4 (- (m_i - 3m_j))) B_{ii}(m_Z^2) \\
& + \frac{(m_i - m_j)}{2} (-m_H^2 + m_Z^2 + P^2) (-m_H^2 (P^2 - 2m_Z^2) - m_H^4 - m_Z^2 (m_Z^2 + P^2) + 2P^4) B_{ij}(P^2) \\
& - \frac{(m_i - m_j)}{2} (-m_Z^4 (P^2 - 3m_H^2) + 2P^2 m_Z^2 (P^2 - m_H^2) + (P^2 - m_H^2)^3 - 2m_Z^6) B_{ij}(m_Z^2) \\
& - (m_i - m_j) (-3m_H^4 (m_Z^2 + P^2) + 4P^2 m_H^2 m_Z^2 + 2m_H^6 + (P^2 - m_Z^2)^2 (m_Z^2 + P^2)) B_{ij}(m_H^2) \\
& - \frac{1}{4} (-m_H^2 + m_Z^2 + P^2) (m_H^4 ((2m_i + m_j) (2m_i (m_j - m_i) + P^2) + m_i m_Z^2) \\
& + m_H^2 (2m_i^2 m_j (P^2 - 2m_Z^2) + m_i (-2m_Z^2 (2m_j^2 + P^2) + 2P^2 m_j^2 + m_Z^4 - P^4) \\
& + 2m_i^3 (4m_Z^2 + P^2) - 2P^2 m_j (3m_j^2 - 2m_Z^2 + P^2)) + m_H^6 (-m_i) \\
& + m_Z^4 (2m_i + m_j) (2m_i (m_j - m_i) + P^2) + P^2 m_Z^2 (-m_i (P^2 - 2m_j^2) + 2m_i^2 m_j + 2m_i^3 \\
& - 2m_j (3m_j^2 + P^2)) + P^2 (6m_j^3 (P^2 - 2m_i^2) - 4m_i m_j^2 (P^2 - 3m_i^2) + m_j (-4P^2 m_i^2 + 6m_i^4 + P^4) \\
& - 6m_i m_j^4 + 2m_i^3 (P^2 - 3m_i^2) + 6m_j^5) - m_i m_Z^6) C_{iji}(P^2) \\
& + \frac{1}{4} (-m_H^2 + m_Z^2 + P^2) (m_Z^4 (m_i (m_H^2 + 4m_j^2 + P^2) + 2m_j (m_H^2 - 3m_j^2 + P^2) + 4m_i^2 m_j - 2m_i^3) \\
& + m_i (P^2 - m_H^2)^2 (m_H^2 + 2(m_i - m_j) (2m_i + m_j) + P^2) - m_Z^2 (-6m_j^3 (m_H^2 + 2m_i^2 + P^2) \\
& + 2m_i m_j^2 (m_H^2 + 6m_i^2 + P^2) + m_j (2m_i^2 (m_H^2 + P^2) + 4P^2 m_H^2 + m_H^4 + 6m_i^4 + P^4) \\
& + 2m_i (m_i^2 (m_H^2 + P^2) - P^2 m_H^2 + m_H^4 - 3m_i^4 + P^4) - 6m_i m_j^4 + 6m_j^5) - m_j m_Z^6) C_{jii}(P^2) \\
& \left. + (m_i - m_j) ((m_H - m_Z)^2 - P^2) ((m_H + m_Z)^2 - P^2) (-m_H^2 + m_Z^2 + P^2) \right\} - (i \leftrightarrow j) \quad (A17)
\end{aligned}$$

$$\begin{aligned}
R_3^Z(Q^2, m_i, m_j) = & \frac{1}{((m_Z + m_H)^2 - P^2)^2 ((m_Z - m_H)^2 - P^2)^2} \left\{ \frac{1}{2} (-m_H^2 + m_Z^2 + P^2) (m_i (m_H^2 (4m_Z^2 + P^2) \right. \\
& - 2m_H^4 + 6P^2 m_j^2 + P^2 m_Z^2 - 2m_Z^4 + P^4) + 3P^2 m_j (-m_H^2 + 2m_j^2 - m_Z^2 + P^2) - 6P^2 m_i^2 m_j \\
& - 6P^2 m_i^3) B_{ii}(P^2) - \frac{1}{2} (-m_H^2 + m_Z^2 + P^2) (-m_Z^2 (-3m_j (m_H^2 + 2m_i^2 + P^2) \\
& + m_i (m_H^2 - 6m_i^2 + P^2) + 6m_i m_j^2 + 6m_j^3) + 2m_i (P^2 - m_H^2)^2 + m_Z^4 (- (m_i + 3m_j))) B_{ii}(m_Z^2) \\
& + \frac{1}{2} (m_i + m_j) (-m_H^2 + m_Z^2 + P^2) (-m_H^2 (P^2 - 2m_Z^2) - m_H^4 - m_Z^2 (m_Z^2 + P^2) + 2P^4) B_{ij}(P^2) \\
& + \frac{1}{2} (m_i + m_j) (m_Z^4 (P^2 - 3m_H^2) + 2P^2 m_Z^2 (m_H^2 - P^2) - (P^2 - m_H^2)^3 + 2m_Z^6) B_{ij}(m_Z^2) \\
& - (m_i + m_j) (-3m_H^4 (m_Z^2 + P^2) + 4P^2 m_H^2 m_Z^2 + 2m_H^6 + (P^2 - m_Z^2)^2 (m_Z^2 + P^2)) B_{ij}(m_H^2) \\
& + \frac{1}{4} (-m_H^2 + m_Z^2 + P^2) (m_H^4 ((2m_i - m_j) (2m_i (m_i + m_j) - P^2) - m_i m_Z^2) \\
& + m_H^2 (2m_i^2 m_j (P^2 - 2m_Z^2) + m_i (2m_Z^2 (2m_j^2 + P^2) - 2P^2 m_j^2 - m_Z^4 + P^4) - 2m_i^3 (4m_Z^2 + P^2) \\
& - 2P^2 m_j (3m_j^2 - 2m_Z^2 + P^2)) + m_H^6 m_i + m_Z^4 (2m_i - m_j) (2m_i (m_i + m_j) - P^2) \\
& + P^2 m_Z^2 (m_i (P^2 - 2m_j^2) + 2m_i^2 m_j - 2m_i^3 - 2m_j (3m_j^2 + P^2)) + P^2 (4m_i m_j^2 (P^2 - 3m_i^2) \\
& + 6m_j^3 (P^2 - 2m_i^2) + m_j (-4P^2 m_i^2 + 6m_i^4 + P^4) + 6m_i m_j^4 - 2P^2 m_i^3 + 6m_i^5 + 6m_j^5) \\
& + m_i m_Z^6) C_{iji}(P^2) + \frac{1}{4} (-m_H^2 + m_Z^2 + P^2) (m_Z^4 (-2m_j (m_H^2 + 2m_i^2 + P^2) \\
& + m_i (m_H^2 - 2m_i^2 + P^2) + 4m_i m_j^2 + 6m_j^3) + m_i (P^2 - m_H^2)^2 (m_H^2 + 2(2m_i - m_j) (m_i + m_j) \\
& + P^2) + m_Z^2 (-2m_i^3 (m_H^2 + 6m_j^2 + P^2) + 2m_i^2 m_j (m_H^2 - 6m_j^2 + P^2) - 2m_i (m_j^2 (m_H^2 + P^2) \\
& - P^2 m_H^2 + m_H^4 - 3m_j^4 + P^4) + m_j (-6m_j^2 (m_H^2 + P^2) + 4P^2 m_H^2 + m_H^4 + 6m_j^4 + P^4) \\
& + 6m_i^4 m_j + 6m_i^5) + m_j m_Z^6) C_{jii}(P^2) \\
& \left. + (m_i + m_j) ((m_H - m_Z)^2 - P^2) ((m_H + m_Z)^2 - P^2) (-m_H^2 + m_Z^2 + P^2) \right\} + (i \leftrightarrow j) \quad (\text{A18})
\end{aligned}$$

$$\begin{aligned}
R_4^Z(Q^2, m_i, m_j) = & \frac{1}{((m_Z + m_H)^2 - P^2)^2 ((m_Z - m_H)^2 - P^2)^2} \left\{ \frac{1}{2} P^2 (2m_Z^2 (m_i (4(m_H^2 + P^2) + 3m_j^2) + 3m_i^2 m_j \right. \\
& - 3m_i^3 - 3m_j^3) - (P^2 - m_H^2) (m_i (-m_H^2 - 6m_j^2 + P^2) + 3m_j (-m_H^2 + 2m_j^2 + P^2) - 6m_i^2 m_j \\
& + 6m_i^3) + m_Z^4 (3m_j - 7m_i) B_{ii}(P^2) + \frac{1}{2} m_Z^2 [2m_Z^2 (3m_j (m_H^2 + m_i^2) + m_i (m_H^2 - 3m_i^2 + 4P^2) \\
& + 3m_i m_j^2 - 3m_j^3) - (P^2 - m_H^2) (-3m_j (m_H^2 + 2m_i^2 + P^2) + m_i (-m_H^2 + 6m_i^2 + 7P^2) \\
& - 6m_i m_j^2 + 6m_j^3) + m_Z^4 (- (m_i + 3m_j))] B_{ii}(m_Z^2) \\
& + \frac{1}{2} P^2 (m_i - m_j) (4m_Z^2 (m_H^2 + P^2) + (P^2 - m_H^2)^2 - 5m_Z^4) B_{ij}(P^2) \\
& + \frac{1}{2} m_Z^2 (m_i - m_j) (m_H^2 (4P^2 - 2m_Z^2) + m_H^4 + 4P^2 m_Z^2 + m_Z^4 - 5P^4) B_{ij}(m_Z^2) \\
& - (m_i - m_j) (m_H^4 (m_Z^2 + P^2) - 2m_H^2 (-4P^2 m_Z^2 + m_Z^4 + P^4) + (P^2 - m_Z^2)^2 (m_Z^2 + P^2)) B_{ij}(m_H^2) \\
& + \frac{1}{4} [m_H^6 (2m_i^2 m_j - m_i (4m_Z^2 + 3P^2) - 2m_i^3 + P^2 m_j) + m_H^4 (m_Z^2 (-6m_i^2 m_j - P^2 m_i \\
& + 6m_i^3 + 3P^2 m_j) + P^2 (m_i - m_j) (4m_i m_j + 4m_i^2 + 6m_j^2 + 3P^2) + 6m_i m_Z^4) \\
& + m_H^2 (m_Z^4 (6m_i^2 m_j + 5P^2 m_i - 6m_i^3 - 3P^2 m_j) + 4P^2 m_Z^2 (m_i - m_j) (-2m_i m_j - 3m_i^2 + P^2) \\
& - P^2 (2m_i^3 (P^2 - 6m_j^2) + 6m_i^2 m_j (2m_j^2 + P^2) + m_i (4P^2 m_j^2 + 6m_j^4 + P^4) - 6m_i^4 m_j + 6m_i^5 \\
& - 3m_j (4P^2 m_j^2 + 2m_j^4 + P^4)) - 4m_i m_H^6) + m_Z^8 m_i - m_Z^6 (m_j (2m_i^2 + P^2) + m_i (P^2 - 2m_i^2)) \\
& - P^2 m_Z^4 (m_i - m_j) (-4m_i m_j - 8m_i^2 + 6m_j^2 + P^2) + P^2 m_Z^2 (-2m_i^3 (6m_j^2 + 5P^2) \\
& + 2m_i^2 m_j (6m_j^2 + P^2) + m_i (8P^2 m_j^2 + 6m_j^4 + P^4) - 6m_i^4 m_j + 6m_i^5 + m_j (P^4 - 6m_j^4)) \\
& + P^4 (2(m_i - m_j) (2P^2 m_i m_j + 3m_j^2 (P^2 - 2m_i^2) + 3m_i^4 + 3m_j^4) - P^4 m_j) + m_i m_Z^8] C_{ijj}(P^2) \\
& + \frac{1}{4} [m_Z^6 (m_i (-m_H^2 + 2m_j^2 + P^2) + m_j (3m_H^2 - 6m_j^2 + P^2) + 4m_i^2 m_j) \\
& + m_i (P^2 - m_H^2)^3 (-m_H^2 + 2m_i (m_i - m_j) + P^2) - m_Z^4 (m_i - m_j) (2m_H^2 (4m_i m_j + m_i^2 + 6m_j^2 \\
& - 2P^2) - 3m_H^4 + 8P^2 m_i m_j + 2m_i^2 (6m_j^2 + 5P^2) - 6m_i^4 - 6m_j^4 + P^4) \\
& - m_Z^2 (P^2 - m_H^2) (-6m_j^3 (m_H^2 + 2m_i^2 + P^2) + 2m_i m_j^2 (m_H^2 + 6m_i^2 + 5P^2) \\
& + m_j (4P^2 m_H^2 + m_H^4 + 4P^2 m_i^2 + 6m_i^4 + P^4) + m_i (4m_H^2 (m_i^2 - P^2) - 3m_H^4 - 8P^2 m_i^2 \\
& - 6m_i^4 + P^4) - 6m_i m_j^4 + 6m_j^5) - m_j m_Z^8] C_{jii}(P^2) \\
& \left. (m_i - m_j) ((m_H - m_Z)^2 - P^2) ((m_H + m_Z)^2 - P^2) (-m_H^2 + m_Z^2 + P^2) \right\} - (i \leftrightarrow j) \quad (A19)
\end{aligned}$$

The functions $T_{1,2,3,4}^V$ ($V = H, Z$) for contributions of Type II are given as follows:

$$\begin{aligned}
T_1^H(Q^2, m_i, m_j) = & \frac{1}{Q^2 (Q^2 - 4m_Z^2)} \left\{ 2(m_Z^2 (m_i + m_j) - Q^2 m_i) B_{ii}(m_Z^2) + 2Q^2 (m_j - m_i) [B_{ij}(m_Z^2) - 2B_{ij}(Q^2)] \right. \\
& \left. , (2m_i^2 - 2m_j^2 + Q^2) (Q^2 m_i - m_Z^2 (m_i + m_j)) C_{iij}(Q^2) \right\} - (i \leftrightarrow j), \quad (A20)
\end{aligned}$$

$$\begin{aligned}
T_2^H(Q^2, m_i, m_j) = & \frac{1}{Q^2 (Q^2 - 4m_Z^2)} \left\{ 2m_Z^2 (m_i - m_j) B_{ii}(m_Z^2) + [m_Z^2 (m_i (2m_j^2 + 3Q^2) + 2m_i^2 m_j - 2m_i^3 \right. \\
& \left. + m_j (Q^2 - 2m_j^2)) - Q^4 m_i] C_{iij}(Q^2) \right\} + (i \leftrightarrow j), \quad (A21)
\end{aligned}$$

$$T_3^H(Q^2, m_i, m_j) = \frac{1}{Q^2(Q^2 - 4m_Z^2)} \left\{ 2m_Z^2(m_i + m_j) B_{ii}(m_Z^2) + [m_Z^2(-m_j(2m_i^2 + Q^2) + 2m_i m_j^2 + 3Q^2 m_i - 2m_i^3 + 2m_j^3) - Q^4 m_i] C_{ijj}(Q^2) \right\} - (i \leftrightarrow j), \quad (\text{A22})$$

$$T_4^H(Q^2, m_i, m_j) = \frac{1}{Q^2(Q^2 - 4m_Z^2)} \left\{ -2(m_Z^2(m_j - m_i) + Q^2 m_i) B_{ii}(m_Z^2) - 2Q^2(m_i + m_j) [B_{ij}(m_Z^2) - 2B_{ij}(Q^2)] \right. \\ \left. , + (2m_i^2 - 2m_j^2 + Q^2)(m_Z^2(m_j - m_i) + Q^2 m_i) C_{ijj}(Q^2) \right\} + (i \leftrightarrow j), \quad (\text{A23})$$

$$T_1^Z(Q^2, m_i, m_j) = \frac{1}{((m_H - m_Z)^2 - P^2)((m_H + m_Z) - P^2)} \left\{ (m_i(m_Z^2 - m_H^2) + P^2 m_j) B_{ii}(P^2) \right. \\ + (m_i(P^2 - m_H^2) + m_j m_Z^2) B_{ii}(m_Z^2) - \frac{1}{2}(m_i - m_j)(m_H^2 - m_Z^2 + P^2) B_{ij}(P^2) \\ + \frac{1}{2}(m_i - m_j)(-m_H^2 - m_Z^2 + P^2) B_{ij}(m_Z^2) + 2m_H^2(m_i - m_j) B_{ij}(m_H^2) \\ + \frac{1}{4}(-m_H^2 - 2m_i^2 + 2m_j^2 - m_Z^2 + P^2)(m_i(m_Z^2 - m_H^2) + P^2 m_j) C_{iji}(P^2) \\ \left. - \frac{1}{4}(m_H^2 + 2m_i^2 - 2m_j^2 - m_Z^2 + P^2)(m_i(P^2 - m_H^2) + m_j m_Z^2) C_{jii}(P^2) \right\} - (i \leftrightarrow j), \quad (\text{A24})$$

$$T_2^Z(Q^2, m_i, m_j) = \frac{1}{((m_H - m_Z)^2 - P^2)((m_H + m_Z) - P^2)} \left\{ P^2(m_i - m_j) B_{ii}(P^2) + m_Z^2(m_i - m_j) B_{ii}(m_Z^2) \right. \\ + \frac{1}{4} \left[m_H^2(P^2(m_i + m_j) + 2m_i m_Z^2) + m_H^4(-m_i) + P^2 m_Z^2(m_i + m_j) \right. \\ \left. - P^2(2(m_i - m_j)^2(m_i + m_j) + P^2 m_j) - m_i m_Z^4 \right] C_{iji}(P^2) \\ + \frac{1}{4} \left[m_Z^2(m_i + m_j)(m_H^2 - 2(m_i - m_j)^2 + P^2) - m_i(P^2 - m_H^2)^2 - m_j m_Z^4 \right] C_{jii}(P^2) \left. \right\} \\ + (i \leftrightarrow j), \quad (\text{A25})$$

$$T_3^Z(Q^2, m_i, m_j) = \frac{1}{((m_H - m_Z)^2 - P^2)((m_H + m_Z) - P^2)} \left\{ P^2(m_i + m_j) B_{ii}(P^2) + m_Z^2(m_i + m_j) B_{ii}(m_Z^2) \right. \\ + \frac{1}{4} \left[m_H^2(m_i(2m_Z^2 + P^2) - P^2 m_j) + m_H^4(-m_i) + P^2 m_Z^2(m_i - m_j) \right. \\ \left. + P^2(P^2 m_j - 2(m_i - m_j)(m_i + m_j)^2) - m_i m_Z^4 \right] C_{iji}(P^2) \\ + \frac{1}{4} \left[m_Z^2(m_i - m_j)(m_H^2 - 2(m_i + m_j)^2 + P^2) - m_i(P^2 - m_H^2)^2 + m_j m_Z^4 \right] C_{jii}(P^2) \left. \right\} \\ - (i \leftrightarrow j), \quad (\text{A26})$$

$$\begin{aligned}
T_4^Z(Q^2, m_i, m_j) = & \frac{1}{((m_H - m_Z)^2 - P^2)((m_H + m_Z) - P^2)} \left\{ - (m_i (m_H^2 - m_Z^2) + P^2 m_j) B_{ii}(P^2) \right. \\
& + (m_i (P^2 - m_H^2) - m_j m_Z^2) B_{ii}(m_Z^2) - \frac{1}{2} (m_i + m_j) (m_H^2 - m_Z^2 + P^2) B_{ij}(P^2) \\
& + \frac{1}{2} (m_i + m_j) (-m_H^2 - m_Z^2 + P^2) B_{ij}(m_Z^2) + 2m_H^2 (m_i + m_j) B_{ij}(m_H^2) \\
& - \frac{1}{4} (-m_H^2 - 2m_i^2 + 2m_j^2 - m_Z^2 + P^2) (m_i (m_H^2 - m_Z^2) + P^2 m_j) C_{iji}(P^2) \\
& \left. - \frac{1}{4} \text{ga} (m_H^2 + 2m_i^2 - 2m_j^2 - m_Z^2 + P^2) (m_i (P^2 - m_H^2) - m_j m_Z^2) C_{jii}(P^2) \right\} + (i \leftrightarrow j), \quad (\text{A27})
\end{aligned}$$

-
- [1] S. Chatrchyan *et al.* (CMS), Observation of a New Boson at a Mass of 125 GeV with the CMS Experiment at the LHC, *Phys. Lett. B* **716**, 30 (2012), arXiv:1207.7235 [hep-ex].
- [2] G. Aad *et al.* (ATLAS), Observation of a new particle in the search for the Standard Model Higgs boson with the ATLAS detector at the LHC, *Phys. Lett. B* **716**, 1 (2012), arXiv:1207.7214 [hep-ex].
- [3] F. Englert and R. Brout, Broken symmetry and the mass of gauge vector mesons, *Phys. Rev. Lett.* **13**, 321 (1964).
- [4] G. S. Guralnik, C. R. Hagen, and T. W. B. Kibble, Global conservation laws and massless particles, *Phys. Rev. Lett.* **13**, 585 (1964).
- [5] P. W. Higgs, Broken symmetries and the masses of gauge bosons, *Phys. Rev. Lett.* **13**, 508 (1964).
- [6] G. Aad *et al.* (ATLAS), A detailed map of Higgs boson interactions by the ATLAS experiment ten years after the discovery, *Nature* **607**, 52 (2022), [Erratum: *Nature* 612, E24 (2022)], arXiv:2207.00092 [hep-ex].
- [7] A. Tumasyan *et al.* (CMS), A portrait of the Higgs boson by the CMS experiment ten years after the discovery., *Nature* **607**, 60 (2022), [Erratum: *Nature* 623, (2023)], arXiv:2207.00043 [hep-ex].
- [8] A. Tumasyan *et al.* (CMS), Search for Higgs boson decays to a Z boson and a photon in proton-proton collisions at $\sqrt{s} = 13$ TeV, *JHEP* **05**, 233, arXiv:2204.12945 [hep-ex].
- [9] G. Aad *et al.* (ATLAS, CMS), Evidence for the Higgs Boson Decay to a Z Boson and a Photon at the LHC, *Phys. Rev. Lett.* **132**, 021803 (2024), arXiv:2309.03501 [hep-ex].
- [10] A. Tumasyan *et al.* (CMS), Measurement of the Higgs boson width and evidence of its off-shell contributions to ZZ production, *Nature Phys.* **18**, 1329 (2022), arXiv:2202.06923 [hep-ex].
- [11] G. Aad *et al.* (ATLAS), Evidence of off-shell Higgs boson production from ZZ leptonic decay channels and constraints on its total width with the ATLAS detector, *Phys. Lett. B* **846**, 138223 (2023), arXiv:2304.01532 [hep-ex].
- [12] F. Caola and K. Melnikov, Constraining the Higgs boson width with ZZ production at the LHC, *Phys. Rev. D* **88**, 054024 (2013), arXiv:1307.4935 [hep-ph].
- [13] J. M. Campbell, R. K. Ellis, and C. Williams, Bounding the Higgs Width at the LHC Using Full Analytic Results for $gg \rightarrow e^- e^+ \mu^- \mu^+$, *JHEP* **04**, 060, arXiv:1311.3589 [hep-ph].
- [14] J. A. Aguilar-Saavedra, A. Bernal, J. A. Casas, and J. M. Moreno, Testing entanglement and Bell inequalities in $H \rightarrow ZZ$, *Phys. Rev. D* **107**, 016012 (2023), arXiv:2209.13441 [hep-ph].
- [15] A. Bernal, P. Caban, and J. Rembieliński, Entanglement and Bell inequalities violation in $H \rightarrow ZZ$ with anomalous coupling, *Eur. Phys. J. C* **83**, 1050 (2023), arXiv:2307.13496 [hep-ph].
- [16] J. A. Aguilar-Saavedra, Tripartite entanglement in $H \rightarrow ZZ, WW$ decays, *Phys. Rev. D* **109**, 113004 (2024), arXiv:2403.13942 [hep-ph].
- [17] A. Bernal, P. Caban, and J. Rembieliński, Entanglement and Bell inequality violation in vector diboson systems produced in decays of spin-0 particles, (2024), arXiv:2405.16525 [hep-ph].
- [18] M. Sullivan, Constraining New Physics with $h \rightarrow VV$ Tomography, (2024), arXiv:2410.10980 [hep-ph].
- [19] B. A. Kniehl, Radiative corrections for $H \rightarrow ZZ$ in the standard model, *Nucl. Phys. B* **352**, 1 (1991).
- [20] K. H. Phan, D. T. Tran, and A. T. Nguyen, One-loop off-shell decay $H^* \rightarrow ZZ$ at future colliders, *Commun. in Phys.* **33**, 369 (2023), arXiv:2209.12410 [hep-ph].
- [21] A. I. Hernández-Juárez, G. Tavares-Velasco, and A. Fernández-Télez, New evaluation of the HZZ coupling: Direct bounds on anomalous contributions and CP-violating effects via a new asymmetry, *Phys. Rev. D* **107**, 115031 (2023), arXiv:2301.13127 [hep-ph].
- [22] A. Soni and R. M. Xu, Probing CP violation via Higgs decays to four leptons, *Phys. Rev. D* **48**, 5259 (1993), arXiv:hep-ph/9301225.
- [23] S. Bolognesi, Y. Gao, A. V. Gritsan, K. Melnikov, M. Schulze, N. V. Tran, and A. Whitbeck, On the Spin and Parity of a Single-Produced Resonance at the LHC, *Phys. Rev. D* **86**, 095031 (2012), arXiv:1208.4018 [hep-ph].
- [24] I. Anderson *et al.*, Constraining Anomalous HVV Interactions at Proton and Lepton Colliders, *Phys. Rev. D* **89**, 035007 (2014), arXiv:1309.4819 [hep-ph].

- [25] B. Şahin, Search for the anomalous ZZH couplings at the CLIC, *Mod. Phys. Lett. A* **34**, 1950299 (2019).
- [26] A. V. Gritsan, J. Roskes, U. Sarica, M. Schulze, M. Xiao, and Y. Zhou, New features in the JHU generator framework: constraining Higgs boson properties from on-shell and off-shell production, *Phys. Rev. D* **102**, 056022 (2020), arXiv:2002.09888 [hep-ph].
- [27] D. Gonçalves, T. Han, S. Ching Iris Leung, and H. Qin, Off-shell Higgs couplings in $H^* \rightarrow ZZ \rightarrow \ell\ell\nu\nu$, *Phys. Lett. B* **817**, 136329 (2021), arXiv:2012.05272 [hep-ph].
- [28] A. Azatov *et al.*, Off-shell Higgs Interpretations Task Force: Models and Effective Field Theories Subgroup Report 10.17181/LHCHWG-2022-001 (2022), arXiv:2203.02418 [hep-ph].
- [29] A. T. Nguyen, D. T. Tran, and K. H. Phan, Effects of one-loop on-shell and off-shell decay $H^* \rightarrow VV$ at future lepton colliders, *J. Phys. Conf. Ser.* **2485**, 012001 (2023), arXiv:2209.13153 [hep-ph].
- [30] B. A. Kniehl, Radiative corrections for associated ZH production at future e^+e^- colliders, *Z. Phys. C* **55**, 605 (1992).
- [31] K. Hagiwara and M. L. Stong, Probing the scalar sector in $e^+e^- \rightarrow f \text{ anti-}f H$, *Z. Phys. C* **62**, 99 (1994), arXiv:hep-ph/9309248.
- [32] K. Hagiwara, S. Ishihara, J. Kamoshita, and B. A. Kniehl, Prospects of measuring general Higgs couplings at e^+e^- linear colliders, *Eur. Phys. J. C* **14**, 457 (2000), arXiv:hep-ph/0002043.
- [33] B. A. Kniehl, Theoretical aspects of standard model Higgs boson physics at a future e^+e^- linear collider, *Int. J. Mod. Phys. A* **17**, 1457 (2002), arXiv:hep-ph/0112023.
- [34] S. S. Biswal, R. M. Godbole, R. K. Singh, and D. Choudhury, Signatures of anomalous VVH interactions at a linear collider, *Phys. Rev. D* **73**, 035001 (2006), [Erratum: *Phys.Rev.D* **74**, 039904 (2006)], arXiv:hep-ph/0509070.
- [35] D. Choudhury and Mamta, Anomalous Higgs Couplings at an e gamma Collider, *Phys. Rev. D* **74**, 115019 (2006), arXiv:hep-ph/0608293.
- [36] R. M. Godbole, D. J. Miller, and M. M. Muhlleitner, Aspects of CP violation in the H ZZ coupling at the LHC, *JHEP* **12**, 031, arXiv:0708.0458 [hep-ph].
- [37] S. Dutta, K. Hagiwara, and Y. Matsumoto, Measuring the Higgs-Vector boson Couplings at Linear e^+e^- Collider, *Phys. Rev. D* **78**, 115016 (2008), arXiv:0808.0477 [hep-ph].
- [38] S. D. Rindani and P. Sharma, Angular distributions as a probe of anomalous ZZH and gammaZH interactions at a linear collider with polarized beams, *Phys. Rev. D* **79**, 075007 (2009), arXiv:0901.2821 [hep-ph].
- [39] I. T. Cakir, O. Cakir, A. Senol, and A. T. Tasci, Probing Anomalous HZZ Couplings at the LHeC, *Mod. Phys. Lett. A* **28**, 1350142 (2013), arXiv:1304.3616 [hep-ph].
- [40] K. Rao, S. D. Rindani, and P. Sarmah, Probing anomalous gauge-Higgs couplings using Z boson polarization at e^+e^- colliders, *Nucl. Phys. B* **950**, 114840 (2020), arXiv:1904.06663 [hep-ph].
- [41] S. Kumar, P. Poulose, R. Rahaman, and R. K. Singh, Measuring Higgs self-couplings in the presence of VVH and VVHH at the ILC, *Int. J. Mod. Phys. A* **34**, 1950094 (2019), arXiv:1905.06601 [hep-ph].
- [42] K. Rao, S. D. Rindani, and P. Sarmah, Study of anomalous gauge-Higgs couplings using Z boson polarization at LHC, *Nucl. Phys. B* **964**, 115317 (2021), arXiv:2009.00980 [hep-ph].
- [43] L. Chen, G. Heinrich, S. P. Jones, M. Kerner, J. Klappert, and J. Schlenk, ZH production in gluon fusion: two-loop amplitudes with full top quark mass dependence, *JHEP* **03**, 125, arXiv:2011.12325 [hep-ph].
- [44] W. Bizoń, F. Caola, K. Melnikov, and R. Röntsch, Anomalous couplings in associated VH production with Higgs boson decay to massive b quarks at NNLO in QCD, *Phys. Rev. D* **105**, 014023 (2022), arXiv:2106.06328 [hep-ph].
- [45] P. Sharma and A. Shivaji, Probing non-standard HVV (V = W, Z) couplings in single Higgs production at future electron-proton collider, *JHEP* **10**, 108, arXiv:2207.03862 [hep-ph].
- [46] K. Rao, S. D. Rindani, P. Sarmah, and B. Singh, Polarized Z cross sections in Higgsstrahlung for the determination of anomalous ZZH couplings, (2022), arXiv:2202.10215 [hep-ph].
- [47] P. Bittar and G. Burdman, Form Factors in Higgs Couplings from Physics Beyond the Standard Model, (2022), arXiv:2204.07094 [hep-ph].
- [48] A. V. Gritsan *et al.*, Snowmass White Paper: Prospects of CP-violation measurements with the Higgs boson at future experiments, (2022), arXiv:2205.07715 [hep-ex].
- [49] X. Chen, X. Guan, C.-Q. He, Z. Li, X. Liu, and Y.-Q. Ma, Complete two-loop electroweak corrections to $e^+e^- \rightarrow HZ$, (2022), arXiv:2209.14953 [hep-ph].
- [50] A. Djouadi, J. Kalinowski, and M. Spira, Hdecay: a program for higgs boson decays in the standard model and its supersymmetric extension, *Computer Physics Communications* **108**, 56774 (1998).
- [51] A. Bredenstein, A. Denner, S. Dittmaier, and M. M. Weber, Precise predictions for the higgs-boson decay $h \rightarrow ww/zz \rightarrow 4$ leptons, *Phys. Rev. D* **74**, 013004 (2006).
- [52] K. Hagiwara, R. D. Peccei, D. Zeppenfeld, and K. Hikasa, Probing the Weak Boson Sector in $e^+e^- \rightarrow W^+W^-$, *Nucl. Phys. B* **282**, 253 (1987).
- [53] D. Chang, W.-K. Keung, and I. Phillips, CP violation in top pair production at an e^+e^- collider, *Nuclear Physics B* **408**, 286 (1993), arXiv:hep-ph/9209267.
- [54] B. Grzadkowski, CP violation in $H \rightarrow t\bar{t}$ decays at e^+e^- colliders, *Phys. Lett. B* **338**, 71 (1994), arXiv:hep-ph/9404330.
- [55] Q.-H. Cao, B. Yan, C. P. Yuan, and Y. Zhang, Probing $Zt\bar{t}$ couplings using Z boson polarization in ZZ production at hadron colliders, *Phys. Rev. D* **102**, 055010 (2020), arXiv:2004.02031 [hep-ph].
- [56] A. I. Hernández-Juárez, R. Gaitán, and G. Tavares-Velasco, Polarized and unpolarized off-shell $H^* \rightarrow ZZ \rightarrow 4\ell$ decay above the $2m_Z$ threshold*, *Chin. Phys. C* **48**, 113103 (2024), arXiv:2402.18497 [hep-ph].
- [57] A. Ballestrero, E. Maina, and G. Pelliccioli, Polarized vector boson scattering in the fully leptonic WZ and ZZ channels at the LHC, *JHEP* **09**, 087, arXiv:1907.04722 [hep-ph].

- [58] E. Maina, Vector boson polarizations in the decay of the Standard Model Higgs, *Phys. Lett. B* **818**, 136360 (2021), arXiv:2007.12080 [hep-ph].
- [59] E. Maina and G. Pelliccioli, Polarized Z bosons from the decay of a Higgs boson produced in association with two jets at the LHC, *Eur. Phys. J. C* **81**, 989 (2021), arXiv:2105.07972 [hep-ph].
- [60] M. Javurkova, R. Ruiz, R. C. L. de Sá, and J. Sandesara, Polarized ZZ pairs in gluon fusion and vector boson fusion at the LHC, *Phys. Lett. B* **855**, 138787 (2024), arXiv:2401.17365 [hep-ph].
- [61] M. Grossi, G. Pelliccioli, and A. Vicini, From angular coefficients to quantum observables: a phenomenological appraisal in di-boson systems, (2024), arXiv:2409.16731 [hep-ph].
- [62] G. Aad *et al.* (ATLAS), Evidence of pair production of longitudinally polarised vector bosons and study of CP properties in $ZZ \rightarrow 4l$ events with the ATLAS detector at $\sqrt{s} = 13$ TeV, *JHEP* **12**, 107, arXiv:2310.04350 [hep-ex].
- [63] G. Aad *et al.* (ATLAS), Observation of gauge boson joint-polarisation states in $W \pm Z$ production from pp collisions at $\sqrt{s} = 13$ TeV with the ATLAS detector, *Phys. Lett. B* **843**, 137895 (2023), arXiv:2211.09435 [hep-ex].
- [64] R. Aaij *et al.* (LHCb), First Measurement of the $Z \rightarrow \mu + \mu -$ Angular Coefficients in the Forward Region of pp Collisions at $\sqrt{s} = 13$ TeV, *Phys. Rev. Lett.* **129**, 091801 (2022), arXiv:2203.01602 [hep-ex].
- [65] G. Aad *et al.* (ATLAS), Measurement of the angular coefficients in Z-boson events using electron and muon pairs from data taken at $\sqrt{s} = 8$ TeV with the ATLAS detector, *JHEP* **08**, 159, arXiv:1606.00689 [hep-ex].
- [66] G. Aad *et al.* (ATLAS), A precise measurement of the Z-boson double-differential transverse momentum and rapidity distributions in the full phase space of the decay leptons with the ATLAS experiment at $\sqrt{s} = 8$ TeV, *Eur. Phys. J. C* **84**, 315 (2024), arXiv:2309.09318 [hep-ex].
- [67] V. Khachatryan *et al.* (CMS), Angular coefficients of Z bosons produced in pp collisions at $\sqrt{s} = 8$ TeV and decaying to $\mu^+ \mu^-$ as a function of transverse momentum and rapidity, *Phys. Lett. B* **750**, 154 (2015), arXiv:1504.03512 [hep-ex].
- [68] A. M. Sirunyan *et al.* (CMS), Measurements of production cross sections of polarized same-sign W boson pairs in association with two jets in proton-proton collisions at $\sqrt{s} = 13$ TeV, *Phys. Lett. B* **812**, 136018 (2021), arXiv:2009.09429 [hep-ex].
- [69] S. Chatrchyan *et al.* (CMS), Measurement of the Polarization of W Bosons with Large Transverse Momenta in W+Jets Events at the LHC, *Phys. Rev. Lett.* **107**, 021802 (2011), arXiv:1104.3829 [hep-ex].
- [70] G. Aad *et al.* (ATLAS), Measurement of the polarisation of W bosons produced with large transverse momentum in pp collisions at $\sqrt{s} = 7$ TeV with the ATLAS experiment, *Eur. Phys. J. C* **72**, 2001 (2012), arXiv:1203.2165 [hep-ex].
- [71] M. Aaboud *et al.* (ATLAS), Measurement of $W^\pm Z$ production cross sections and gauge boson polarisation in pp collisions at $\sqrt{s} = 13$ TeV with the ATLAS detector, *Eur. Phys. J. C* **79**, 535 (2019), arXiv:1902.05759 [hep-ex].
- [72] V. Khachatryan *et al.* (CMS), Measurement of the W boson helicity fractions in the decays of top quark pairs to lepton + jets final states produced in pp collisions at $\sqrt{s} = 8$ TeV, *Phys. Lett. B* **762**, 512 (2016), arXiv:1605.09047 [hep-ex].
- [73] M. Aaboud *et al.* (ATLAS), Measurement of the W boson polarisation in $t\bar{t}$ events from pp collisions at $\sqrt{s} = 8$ TeV in the lepton + jets channel with ATLAS, *Eur. Phys. J. C* **77**, 264 (2017), [Erratum: *Eur.Phys.J.C* 79, 19 (2019)], arXiv:1612.02577 [hep-ex].
- [74] G. Aad *et al.* (CMS, ATLAS), Combination of the W boson polarization measurements in top quark decays using ATLAS and CMS data at $\sqrt{s} = 8$ TeV, *JHEP* **08** (08), 051, arXiv:2005.03799 [hep-ex].
- [75] G. Aad *et al.* (ATLAS), Measurement of the polarisation of W bosons produced in top-quark decays using dilepton events at $\sqrt{s} = 13$ TeV with the ATLAS experiment, *Phys. Lett. B* **843**, 137829 (2023), arXiv:2209.14903 [hep-ex].
- [76] D. Buarque Franzosi, O. Mattelaer, R. Ruiz, and S. Shil, Automated predictions from polarized matrix elements, *JHEP* **04**, 082, arXiv:1912.01725 [hep-ph].
- [77] M. Hoppe, M. Schönherr, and F. Siegert, Polarised cross sections for vector boson production with SHERPA, (2023), arXiv:2310.14803 [hep-ph].
- [78] G. Aad *et al.* (ATLAS), Search for flavor-changing neutral-current couplings between the top quark and the Z boson with proton-proton collisions at $\sqrt{s} = 13$ TeV with the ATLAS detector, *Phys. Rev. D* **108**, 032019 (2023), arXiv:2301.11605 [hep-ex].
- [79] G. Aad *et al.* (ATLAS), Search for flavour-changing neutral tqH interactions with $H \rightarrow \gamma\gamma$ in pp collisions at $\sqrt{s} = 13$ TeV using the ATLAS detector, *JHEP* **12**, 195, arXiv:2309.12817 [hep-ex].
- [80] J. A. Aguilar-Saavedra, Top flavor-changing neutral interactions: Theoretical expectations and experimental detection, *Acta Phys. Polon. B* **35**, 2695 (2004), arXiv:hep-ph/0409342.
- [81] A. I. Hernández-Juárez, G. Tavares-Velasco, and R. Gaitán, Non-diagonal contributions to $Z\gamma V^*$ vertex, polarizations and bounds on $Z\bar{t}q$ couplings, (2022), arXiv:2203.16819 [hep-ph].
- [82] A. I. Hernández-Juárez, R. Gaitán, and R. Martínez, $H \rightarrow Z\gamma$ decay and CP violation, *Phys. Rev. D* **111**, 015001 (2025), arXiv:2405.03094 [hep-ph].
- [83] R. Mertig, M. Bohm, and A. Denner, FEYN CALC: Computer algebraic calculation of Feynman amplitudes, *Comput. Phys. Commun.* **64**, 345 (1991).
- [84] V. Shtabovenko, R. Mertig, and F. Orellana, New Developments in FeynCalc 9.0, *Comput. Phys. Commun.* **207**, 432 (2016), arXiv:1601.01167 [hep-ph].
- [85] V. Shtabovenko, R. Mertig, and F. Orellana, FeynCalc 9.3: New features and improvements, *Comput. Phys. Commun.* **256**, 107478 (2020), arXiv:2001.04407 [hep-ph].
- [86] V. Shtabovenko, R. Mertig, and F. Orellana, FeynCalc 10: Do multiloop integrals dream of computer codes?, *Comput. Phys. Commun.* **306**, 109357 (2025), arXiv:2312.14089 [hep-ph].
- [87] T. Hahn and M. Perez-Victoria, Automated one loop calculations in four-dimensions and D-dimensions, *Comput. Phys. Commun.* **118**, 153 (1999), arXiv:hep-ph/9807565.
- [88] R. E. Cutkosky, Singularities and discontinuities of Feynman amplitudes, *J. Math. Phys.* **1**, 429 (1960).

- [89] A. I. Hernández-Juárez, A. Moyotl, and G. Tavares-Velasco, Bounds on the absorptive parts of the chromomagnetic and chromoelectric dipole moments of the top quark from LHC data, *Eur. Phys. J. Plus* **137**, 925 (2022), arXiv:2109.09978 [hep-ph].
- [90] G. J. Gounaris, J. Layssac, and F. M. Renard, New and standard physics contributions to anomalous Z and gamma selfcouplings, *Phys. Rev. D* **62**, 073013 (2000), arXiv:hep-ph/0003143.
- [91] A. I. Hernández-Juárez, A. Moyotl, and G. Tavares-Velasco, Contributions to ZZV^* ($V = \gamma, Z, Z'$) couplings from CP violating flavor changing couplings, *Eur. Phys. J. C* **81**, 304 (2021), arXiv:2102.02197 [hep-ph].
- [92] A. I. Hernández-Juárez, G. Tavares-Velasco, and A. Moyotl, Chromomagnetic and chromoelectric dipole moments of quarks in the reduced 331 model, *Chin. Phys. C* **45**, 113101 (2021), arXiv:2012.09883 [hep-ph].
- [93] A. I. Hernández-Juárez, A. Moyotl, and G. Tavares-Velasco, New estimate of the chromomagnetic dipole moment of quarks in the standard model, *Eur. Phys. J. Plus* **136**, 262 (2021), arXiv:2009.11955 [hep-ph].